

Occupational Head Protection: Considerations for Test Methods and Use

Maura E. McCartney

Thesis submitted to the faculty of the Virginia Polytechnic Institute and State University in
partial fulfillment of the requirements for the degree of

Master of Science
In
Biomedical Engineering

Steven Rowson, Chair
Francis S. Gayzik
Michael L. Madigan

May 6th, 2021
Blacksburg, VA

Keywords: biomechanics, linear, acceleration, occupational, head injury, construction,
motorsports

Occupational Head Protection: Considerations for Test Methods and Use

Maura E. McCartney

ACADEMIC ABSTRACT

Occupational accidents are a main source of traumatic brain injuries (TBIs), with TBIs accounting for a substantial portion of all work-related deaths. Motor vehicle accidents and falls are consistently leading causes of head injury and fatality across industries. These injuries can have serious long-term consequences on an individual's quality of life and lead to large economic costs within society. This thesis investigated sources of occupational TBI prevention within two industries, construction and professional motorsports. In the last twenty years there have been major safety advancements within these industries, and yet the risk of TBI still exists. There is a need for safety standards that better reflect real-world injury scenarios.

First, this thesis considered improvements to construction hard hat safety standards by evaluating the ability of Type 1 and Type 2 hard hats to reduce head injuries due to falls. Hard hats were evaluated over a range of real-world fall heights and three impact locations, using a twin-wire drop tower. Linear acceleration was used to predict injury risks. Type 2 hard hats substantially reduced skull fracture and concussion risk when compared to Type 1, indicating that if more workers wore Type 2 hard hats the risk of severe head injuries in the construction industry would be reduced. Next, this thesis compared real-world motorsport crash simulations and head impact laboratory tests designed to simulate real-world head impacts. Deformation and change in velocity were used to compare the energy managed by each system. The laboratory results generally tested higher severity impacts, with higher accelerations, compared to the simulations, despite managing a similar amount of energy. This indicates a large amount of the energy involved in the simulations was managed by the surrounding protective systems. The differences between systems create challenges for representing real-world crashes in a laboratory setting. Overall, the comparison in this thesis raises considerations for future helmet testing protocols in order to better match real-world simulations.

Occupational Head Protection: Considerations for Test Methods and Use

Maura E. McCartney

GENERAL AUDIENCE ABSTRACT

Occupational accidents are a main source of traumatic brain injuries (TBIs), with TBIs accounting for a substantial portion of all work-related deaths. Motor vehicle accidents and falls are consistently leading causes of head injury and fatality across industries. These injuries can have serious long-term consequences on an individual's quality of life and lead to large economic costs within society. This thesis investigated sources of occupational TBI prevention within two industries, construction and professional motorsports. In the last twenty years there have been major safety advancements within these industries, and yet the risk of TBI still exists. There is a need for safety standards that better reflect real-world injury scenarios. This thesis considered improvements to construction hard hat safety standards by evaluating the ability of two different hard hat types to reduce head injuries due to falls. It also compared real-world motorsport crash simulations and head impact laboratory tests designed to simulate real-world head impacts. This comparison raises considerations for future helmet testing protocols in order to better represent real-world simulations.

ACKNOWLEDGEMENTS

I would like to thank my advisor, Dr. Steve Rowson, for all of his support and guidance throughout this process. I would also like to thank my committee members, Dr. Madigan and Dr. Gayzik, for their willingness to provide help.

Special thank you to my fellow lab members, Emily Kieffer, Ann Harlos, Summer Keim, and Charlotte Clark, for their friendship and endless support.

I would also like to thank Mark Begonia and Barry Miller, who were always willing to lend a hand or answer my questions while in the lab.

Finally, thank you to all my family and friends for their support and encouragement.

TABLE OF CONTENTS

ACADEMIC ABSTRACT	ii
GENERAL AUDIENCE ABSTRACT.....	iii
ACKNOWLEDGEMENTS.....	iv
TABLE OF CONTENTS.....	v
LIST OF FIGURES	vii
LIST OF TABLES.....	viii
INTRODUCTION	1
References	4
Chapter 1.....	5
Abstract	5
Introduction.....	6
Methods.....	8
Results.....	9
Discussion	15
Conclusion.....	19
References.....	20
Chapter 2.....	21
Abstract	21
Introduction.....	23
Methods.....	25
Simulation Data Reduction.....	28
Laboratory Testing Methods	29
Simulation Deformation Analysis	31
Laboratory Deformation Analysis.....	32
Regression Analysis and Predicted Accelerations.....	33
Results	34
Condition A	34
Simulation and Laboratory Results.....	34
Regression Analysis Results.....	35
Condition B.....	37
Simulation and Laboratory Results.....	37
Regression Analysis Results.....	38
Condition C.....	39

Simulation and Laboratory Results.....	39
Regression Analysis Results.....	40
Condition D.....	42
Simulation and Laboratory Results.....	42
Regression Analysis Results.....	43
Condition E.....	44
Simulation and Laboratory Results.....	44
Regression Analysis Results.....	45
Condition F.....	47
Simulation and Laboratory Results.....	47
Regression Analysis Results.....	48
Condition G.....	49
Simulation and Laboratory Results.....	49
Regression Analysis Results.....	50
Condition H.....	52
Simulation and Laboratory Results.....	52
Regression Analysis Results.....	53
Condition I.....	54
Simulation and Laboratory Results.....	54
Regression Analysis Results.....	55
Condition J.....	57
Simulation and Laboratory Results.....	57
Regression Analysis Results.....	58
Discussion.....	59
Conclusion.....	65
References.....	67
Appendix A: Summary Tables for Simulation and Laboratory Results.....	68

LIST OF FIGURES

Figure 1.1 Fall height distribution for each fall scenario in the 76 accidents analyzed..... 10

Figure 1.2 Peak linear acceleration (PLA) (g) and HIC 15ms for all hard hat models at the rear impact location..... 11

Figure 1.3 Peak linear acceleration (PLA) (g) and HIC 15ms for all hard hat models at the side impact location..... 12

Figure 1.4 Peak linear acceleration (PLA) (g) and HIC 15ms for all hard hat models at the oblique impact location..... 13

Figure 1.5 Skull fracture risk calculated from HIC as a function of impact velocity..... 14

Figure 1.6 Concussion risk as a function of impact velocity..... 15

Figure 2.1 Overview of left side (left) and right side (right) impact locations tested..... 30

Figure 2.2 Acceleration as a function of deformation (left) and as a function of delta V (right) for the 75-degree impact condition..... 36

Figure 2.3 Acceleration as a function of deformation (left) and as a function of delta V (right) for the 54-degree impact condition..... 39

Figure 2.4 Acceleration as a function of deformation (left) and as a function of delta V (right) for the 37-degree impact condition..... 41

Figure 2.5 Acceleration as a function of deformation (left) and as a function of delta V (right) for the 21-degree impact condition..... 44

Figure 2.6 Acceleration as a function of deformation (left) and as a function of delta V (right) for the 15-degree impact condition..... 46

Figure 2.7 Acceleration as a function of deformation (left) and as a function of delta V (right) for the 9-degree impact condition..... 49

Figure 2.8 Acceleration as a function of deformation (left) and acceleration as a function of delta V (right) for the -9-degree impact condition..... 51

Figure 2.9 Acceleration as a function of deformation (left) and acceleration as a function of delta V (right) for the -21-degree impact condition..... 54

Figure 2.10 Acceleration as a function of deformation (left) and acceleration as a function of delta V (right) for the -55-degree impact condition..... 56

Figure 2.11 Acceleration as a function of deformation (left) and acceleration as a function of delta V (right) for the -74-degree impact condition..... 59

LIST OF TABLES

Table 2.1 Comparison of the simulation and laboratory setups.....	27
Table 2.2.a Simulation results for the 75-degree impacts.....	35
Table 2.2.b Laboratory results for the 75-degree impacts.	35
Table 2.2.c Regression analysis results for the 75-degree impacts.....	36
Table 2.3.a Simulation results for the 54-degree impacts.....	37
Table 2.3.b The laboratory testing results for the 54-degree impacts.....	37
Table 2.3.c Regression analysis results for the 54-degree impacts.....	38
Table 2.4.a Simulation results for the 37-degree impacts.....	40
Table 2.4.b The laboratory testing results for the 37-degree impacts.....	40
Table 2.4.c Regression analysis results for the 37-degree impacts.....	41
Table 2.5.a Simulation results for the 21-degree impacts.....	42
Table 2.5.b The laboratory testing results for the 21-degree impacts.....	42
Table 2.5.c Regression analysis results for the 21-degree impacts.....	43
Table 2.6.a Simulation results for the 15-degree impacts.....	45
Table 2.6.b The laboratory testing results for the 15-degree impacts.....	45
Table 2.6.c Regression analysis results for the 15-degree impacts.....	46
Table 2.7.a Simulation results for the 9-degree impacts.....	47
Table 2.7.b The laboratory testing results for the 9-degree impacts.....	47
Table 2.7.c Regression analysis results for the 9-degree impacts.....	48
Table 2.8.a Simulation results for the -9-degree impacts.	50
Table 2.8.b The laboratory testing results for the -9-degree impacts.	50
Table 2.8.c Regression analysis results for the -9-degree impacts.....	51
Table 2.9.a Simulation results for the -21-degree impacts.	52
Table 2.9.b The laboratory testing results for the -21-degree impacts.	52
Table 2.9.c Regression analysis results for the -21-degree impacts.....	53
Table 2.10.a Simulation results for the -55-degree impacts.	55
Table 2.10.b The laboratory testing results for the -55-degree impacts.	55
Table 2.10.c Regression analysis results for the -55-degree impacts.....	56
Table 2.11.a Simulation results for the -74-degree impacts.	57
Table 2.11.b The laboratory testing results for the -74-degree impacts.	57
Table 2.11.c Regression analysis results for the -74-degree impacts.....	58
Table A.1 Summary table of all metrics calculated for the simulation impacts.	68
Table A.2 Summary table of all metrics calculated for the laboratory impacts.....	69

INTRODUCTION

Traumatic brain injuries (TBI) are a major source of injury and fatality among work-related accidents, accounting for approximately 22% of all work-related deaths [1]. Additionally, motor vehicle accidents and falls have consistently been the leading causes of TBI-related death within occupational injuries, with two studies finding them to account for 50-60% of all TBI-related deaths [1, 2]. These injury mechanisms are frequently observed in the construction industry as well as transportation [1-3]. Overall, TBIs can cause a number of immediate symptoms, such as headache and cognitive dysfunction, as well as have long term consequences for individuals suffering from severe injury or with a history of repeated mild TBI [4, 5]. These long-term effects not only reduce quality of life for the individual, but they also create large economic costs within society [2].

Motor vehicle accidents and falls create high-speed impact events with high head injury risks. Specifically, head injuries are caused by a combination of linear and rotational acceleration to the head. High linear accelerations create pressure changes within the brain, resulting in focal damage to the brain, which may include bruising and bleeding, and even skull fracture [5]. Alternatively, rotational accelerations produce shearing forces and strain causing more diffuse damage to brain tissue, such as diffuse axonal injuries [5]. Mild traumatic brain injuries (mTBIs), or concussions, are an example of these diffuse brain injuries. All brain injuries are composed of both translational and rotational components [5], and both components should be considered in injury risk evaluation. However, linear acceleration has traditionally been used more frequently, as safety standards were developed to evaluate severe TBI, such as skull fracture, which is more reliant on translational accelerations. These injury mechanisms are considered when safety

standards are developed, and context surrounding the industry and common injury scenarios must be considered.

Regulatory bodies have made many efforts to understand and reduce injury risk among workers in recent years. For example, the Occupational Safety and Health Administration (OSHA) outlines a number of standards that must be followed to keep workers safe. In the construction industry, they have established a fall protection campaign and require hard hats to meet industrial head protection standards set by the American National Standards Institute (ANSI/ISEA Z89.1-2014 (R2019)). These standards evaluate the ability of head protection to attenuate impact energy during drop tests, as well as evaluate things like penetration and fire resistance [6]. Similarly, there have been many improvements to motor vehicles, such as implementing airbags and improved seat belt restraints, to reduce motor vehicle injuries. Despite efforts to improve safety, there is still a high risk of occupational TBIs and a need for safety standards to better reflect real-world injury scenarios. This thesis will therefore investigate TBI prevention in two occupations, construction and professional motorsports.

First, TBI prevention in the construction industry will be considered. Falls are still the leading cause of injury in the construction industry [1], despite recent efforts to improve fall safety. Construction hard hat design is not optimized for fall protection, but rather focuses on being struck by objects. [6]. Additionally, hard hat types exist to account for different needs. For example, Type 1 models are rated for top impacts, while Type 2 models, which have a secondary EPS foam liner, are rated for top and off-center impacts [6]. Despite this additional level of protection, Type 2 models are not universally required across the industry and are used less often than Type 1 models. Construction hard hat performance will be evaluated between Type 1 and Type 2 models, to understand how their use could reduce head injuries due to falls from height.

Next, TBI prevention within professional motorsports, such as the National Association of Stock Car Racing (NASCAR), will be investigated. NASCAR has a history of high-profile injuries and deaths, many of which involve injury to the head and the craniovertebral junction [7]. In the last 20 years since these injuries, there have been great improvements in safety, including the introduction of the Head and Neck Support (HANS) device, improved barriers, and energy-absorbing impact padding [8]. Improvements have also been made to helmet regulations, through organizations like the Snell Foundation, the SFI Foundation, and the FIA Foundation. These organizations set clear certification requirements that must be met by helmet manufacturers [9, 10]. They evaluate helmet performance based on a number of conditions, including impact attenuation, penetration resistance, fire resistance, and retention system strength [9, 10]. Despite the protective measures implemented, head injury is still a concern due to the high-speed nature of motorsports. Concussions are a common injury within racing [11, 12]. Isolated head impact events, such as the ones used in helmet testing, are not necessarily representative of the complex crashes that occur in racing, which contain multiple impacts and are of much longer duration. It is also becoming common practice for racing teams to modify the helmet with new technology, such as cameras and headsets, to add a competitive advantage. These modifications are not regulated by current helmet standards, meaning any changes to the helmet are done after certification and without safety standards in mind. Therefore, real-world NASCAR crash simulations and laboratory tests designed to simulate real world head impacts will be compared. This comparison will raise considerations for future use in developing a new laboratory test protocol that will include the evaluation of helmet modifications and their effects on helmet performance.

References

- [1] H. M. Tiesman, S. Konda, and J. L. Bell, "The epidemiology of fatal occupational traumatic brain injury in the US," *American journal of preventive medicine*, vol. 41, no. 1, pp. 61-67, 2011.
- [2] J. A. Langlois, W. Rutland-Brown, and M. M. Wald, "The epidemiology and impact of traumatic brain injury: a brief overview," *The Journal of head trauma rehabilitation*, vol. 21, no. 5, pp. 375-378, 2006.
- [3] A. C. Tricco, A. Colantonio, M. Chipman, G. Liss, and B. McLellan, "Work-related deaths and traumatic brain injury," *Brain injury*, vol. 20, no. 7, pp. 719-724, 2006.
- [4] S. P. Broglio *et al.*, "National Athletic Trainers' Association position statement: management of sport concussion," *Journal of athletic training*, vol. 49, no. 2, pp. 245-265, 2014.
- [5] A. K. Ommaya, L. Thibault, and F. A. Bandak, "Mechanisms of impact head injury," *International Journal of Impact Engineering*, vol. 15, no. 4, pp. 535-560, 1994.
- [6] *American National Standards for Industrial Head Protection, ANSI/ISEA Z89.1-2014 (R2019)*, I. American National Standards Institute, Arlington, VA 22, 2014.
- [7] A. Kaul, A. Abbas, G. Smith, S. Manjila, J. Pace, and M. Steinmetz, "A revolution in preventing fatal craniovertebral junction injuries: lessons learned from the Head and Neck Support device in professional auto racing," *Journal of neurosurgery: Spine*, vol. 25, no. 6, pp. 756-761, 2016.
- [8] J. Patalak, T. Gideon, and J. Melvin, "Examination of a properly restrained motorsport occupant," *SAE International journal of transportation safety*, vol. 1, no. 2, pp. 261-277, 2013.
- [9] *SFI Specification 41.1*, I. SFI Foundation, 2013. [Online]. Available: https://www.sfifoundation.com/wp-content/pdfs/specs/Spec_41.1_032713.pdf
- [10] *Special Applications Standard for Protective Headgear: For Use in Competitive Automotive Sports*, I. The Snell Foundation, 2020. [Online]. Available: http://smf.org/standards/sa/2020/SA2020_final.pdf
- [11] N. D. Deakin *et al.*, "Concussion in motor sport: a medical literature review and engineering perspective," *Journal of Concussion*, vol. 1, p. 2059700217733916, 2017.
- [12] O. Minoyama and H. Tsuchida, "Injuries in professional motor car racing drivers at a racing circuit between 1996 and 2000," (in English), *British Journal of Sports Medicine*, vol. 38, no. 5, p. 613, Oct 2004, 2016-04-07 2004, doi: <http://dx.doi.org/10.1136/bjism.2003.007674>.

CHAPTER 1

Evaluation of Hard Hats for the Reduction of Head Injuries due to Falls

Abstract

The construction industry accounts for more fatal traumatic brain injury events (TBIs) than any other industry, with 57% of these related to falls. Despite this, hard hat standards do not focus on fall protection, and Type 2 models, which are rated for off-center impacts, are not frequently used. This study's purpose was to compare fall-related injury risks between Type 1 and Type 2 hard hats. Construction-based accident reports were analyzed using a database provided by OSHA. Analysis considered falls during the construction of buildings associated with head injury. Hard hat performance was then evaluated over a range of low fall heights, 0.3 - 2.4 m, using a twin-wire drop tower system. Three impact locations were tested: rear, side, and oblique. Three Type 1 models and two Type 2 models were tested once at each height. Acceleration and impact velocity were recorded. Peak linear acceleration (PLA) and Head Injury Criterion (HIC) 15 ms were calculated. Skull fracture risk and concussion risk were then calculated for each location. Falls from a ladder or scaffold accounted for 46% of accidents and 42% of fatalities. Fall heights from ladders (3.2 ± 2.1 m) were similar to scaffold fall heights (3.2 ± 1.9 m). Type 2 models had lower PLA and HIC values when compared to Type 1. At 5.7 m/s, Type 2 hard hats reduced skull fracture risk by approximately 64% (oblique), 92% (rear), and 34% (side) compared to Type 1. Concussion risk was reduced by 53% (oblique), 78% (rear), and 2% (side). Type 2 hard hats substantially reduce skull fracture and concussion risk when compared to Type 1 hard hats. These findings indicate that the risk of severe head injuries in the construction industry would be substantially reduced if more workers wore Type 2 hard hats.

Introduction

The construction industry accounts for more fatal traumatic brain injury (TBI) events than any other industry and is responsible for 25% of all work-related TBIs [1]. Additionally, 57% of these TBI fatalities are related to falls [1]. Injuries in the construction industry also have a significant economic and societal impact. Employer spending on workers' compensation in the construction industry is more than twice the average spending for employers in all other industries [2]. The total costs of fatal and nonfatal injuries in the construction industry were estimated to be \$11.5 billion in 2002 [3]. Additionally, one estimate found "falls, slips, and trips" to account for 25% of all construction worker compensation claims [2], and in 2002, falls to a lower level were estimated to result in \$950 million in costs due to days away from work [3]. The days away from work rate in the construction industry is 44% higher than the average rate of all other private industries [2]. However, there has been little reduction in injuries and fatalities due to falls in the construction industry, despite campaigns to increase awareness and improve compliance with safety precautions and fall protection [2].

Hard hats are used in construction to prevent injury to the head, and they are meant to resist penetration by objects, absorb energy from impacts, and protect against electrical hazards [4]. Hard hat standards do not focus on protection from falls despite this being a major source of injury and death in the construction industry. Additionally, there are two classifications of hard hats, Type 1, which are rated for protection from top impacts, and Type 2, which are rated for top and off-center impacts [4]. Most Type 2 designs, therefore, incorporate a foam lining to help absorb energy from the impact. However, Type 1 hard hats are much more common among general construction projects, and Type 2 hard hats are only required for certain occupations. Another safety helmet design has recently been added to the market, which more closely resembles a climbing helmet. It is designed for high elevation tasks, such as electrical work, and is most often classified as a Type

2 model. These helmets replace traditional hard hat design with a design similar to a bike or climbing helmet and include a chin strap, size adjustment, and foam lining throughout the entire helmet. However, there is little research available on hard hat and safety helmet performance. While these nontraditional hard hats seem promising, they are substantially more expensive than traditional models and much less common at construction sites.

Hard hat standards are established by the American National Standards Institute and sets “minimum performance and labeling requirements for protective helmets used in industrial and occupational settings” [4]. It is responsible for classifications of hard hats by location of impact and electrical protection. The standards require both Type 1 and Type 2 models to be evaluated for force transmission and apex penetration, but only Type 2 are tested for impact attenuation and off-center penetration. The impact attenuation performance of Type 1 is not evaluated. Type 2 impact attenuation requirements involve dropping an ISO headform on a hemispherical steel anvil such that the helmet is struck on a location above the headform’s specified dynamic testing line. Only an impact velocity of 3.5 m/s is tested, and the maximum acceleration must not exceed 150g. Fall scenarios within construction accidents may encompass a wide range of fall heights and orientations that are not covered by this testing specification. Therefore, the standards are limited. They do not test Type 1 impact attenuations; they only test Type 2 models for a single, low energy impact. They do not specify the implications of these standards on injury risk.

This study's objective was to evaluate the ability of different hard hat types to reduce head injury risk due to a fall. We hypothesized that Type 2 hard hats would substantially reduce the risk of concussion and skull fracture due to falling if required to be worn across all construction occupations.

Methods

First, a preliminary analysis of construction industry accident reports was conducted to categorize common fall scenarios within the industry. The Fatality and Catastrophe Investigation Summaries database, provided on the Occupational Safety and Health Administration (OSHA) website, was used to conduct the analysis. The search terms used were “fall AND concussion” and “fall AND skull” for accidents occurring during the construction of buildings from January 1st, 2009 to December 31st, 2018. Total accidents, fatalities, the height of the fall, and the fall's nature were recorded.

Hard hat performance was then evaluated over a range of low fall heights, 12” to 96” with 12” increments (0.3 m to 2.4 m), using a drop tower. These low fall heights are commonly reported in construction industry accidents and are heights at which there is a large potential for injury reduction. A twin-wire drop tower was used with a carriage and size J metal ISO headform that totaled 5 kg. The headform was mounted on a ball joint with a single accelerometer positioned at the center of gravity along the z-axis. This allows the headform to be positioned in any orientation and still record the resultant acceleration. Impact velocity was recorded using a velocity detector and a detector flag attached to the carriage. The detector was placed above the anvil at the closest height that allowed clearance by the flag. Velocity recordings from each test at the corresponding height were averaged for the final impact velocity conditions.

This final range of impact velocities was used to represent possible head impact velocities for these low fall heights. There is limited literature on how individuals fall from elevation. It is unknown how likely it would be to impact the body or head first, and how this would affect the head impact velocity. These velocities will therefore indicate trends between hard hat types over a range of potential head impact velocities for low fall heights.

Three impact locations were tested; a rear, side, and oblique surface of the hard hat. The rear and side locations were positioned just above the rim of the hard hat, approximately two inches (0.05 m), and positioned to engage the foam liner in Type 2 models. The oblique location was positioned approximately 45 degrees between the rear and side locations and at a slightly higher elevation toward the crown. This position was on the edge of the foam liner and shell interface of Type 2 models. All hard hats were fitted according to product instructions. Three models of Type 1 hard hats and two models of Type 2 hard hats were each tested one time at each test height. Acceleration and impact velocity were recorded. Hard hat models were not tested beyond heights at which the corresponding impact acceleration exceeded 400 g. Acceleration data were filtered according to ANSI Z89.1 standards, which require compliance with SAE Recommended Practice J211, Channel Frequency Class 1000. Peak linear acceleration (PLA) and Head Injury Criterion (HIC) 15 ms were then calculated. Average skull fracture risk was calculated based on HIC for each hard hat type and location [5-7]. Average concussion risk was also calculated for each type and location [8].

Results

76 of the 88 accident reports included had enough information for analysis. Figure 1 shows the distribution of fall heights based on the surface the individual fell from for all 76 cases. The highest fall heights were associated with elevated floor, while the lowest heights were associated with ladders and scaffolds. Falls from a ladder or scaffold accounted for 46% of all falls and 42% of all fatalities. The distribution of fall heights from ladders (3.2 ± 2.1 m) is similar to scaffold fall heights (3.2 ± 1.9 m). The median and interquartile ranges from ladder falls were 2.4 [1.8 – 4.5] m, while the median and interquartile ranges for scaffold falls were 2.2 [1.8 – 4.4] m.

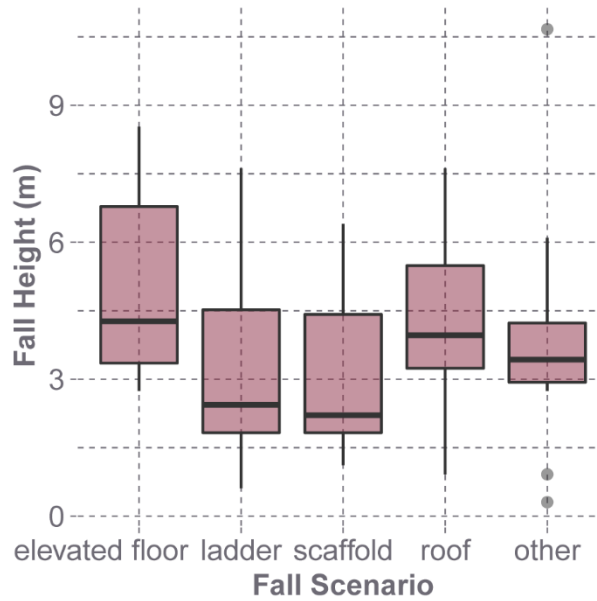


Figure 1.1 Fall height distribution for each fall scenario in the 76 accidents analyzed. The highest fall heights were associated with elevated floor, while the lowest heights were associated with ladders and scaffolds. The distribution of fall heights from ladders and scaffolds are similar.

The impact velocities tested were: 2.1, 3.1, 4.0, 4.7, 5.3, 5.7, 6.2, 6.6 (m/s). The average coefficient of variation for the impact velocities was $1.6\% \pm 0.9\%$. For the rear drop tests, both PLA and HIC were lower for Type 2 hard hats compared to Type 1 (Figure 2). All Type 1 models exceeded 400 g before 5.3 m/s, which corresponded to a drop height of 1.5 m. At 5.3 m/s, Type 2 models were under 200 g, and they experienced PLA values less than 250 g at 6.6 m/s. Similarly, all Type 1 models had HIC values exceeding 2000 at or before 5.3 m/s, while the Type 2 models never reached a HIC value of 2000.

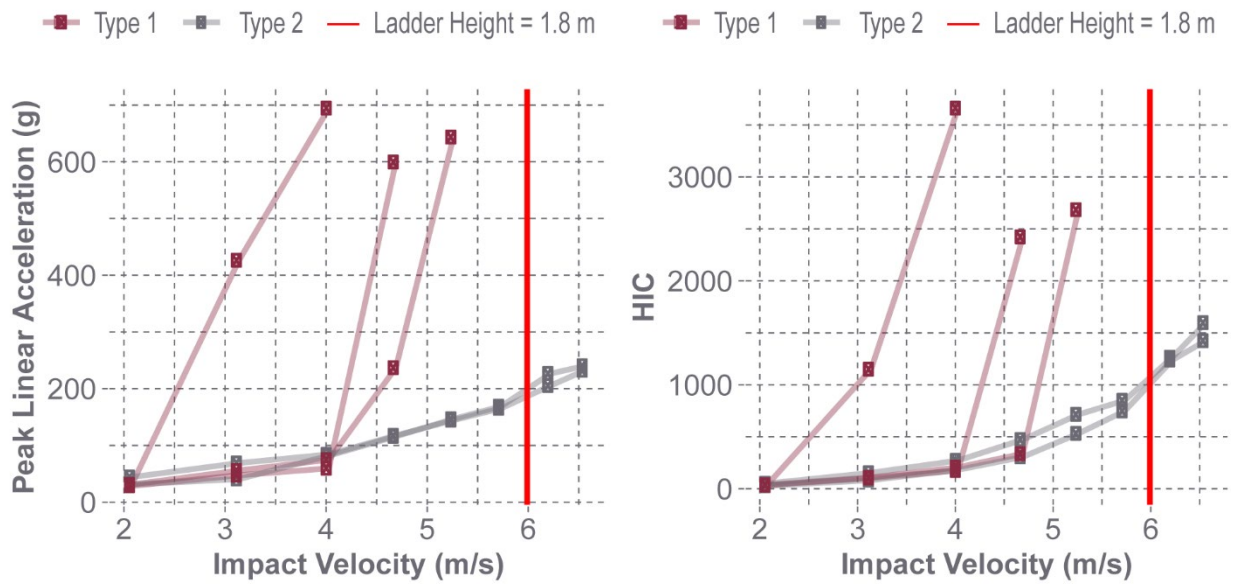


Figure 1.2 Peak linear acceleration (PLA) (g) and HIC 15ms for all hard hat models at the rear impact location. Both PLA and HIC were lower for Type 2 hard hats compared to Type 1. “Ladder Height” corresponds to a theoretical velocity of 6.0 m/s and fall height of 1.8 m, which is the 25th percentile fall height from ladders. All 3 Type 1 models exceeded 400 g before 1.8 m.

For the side impact locations, PLA and HIC were again less for Type 2 hard hats compared to Type 1 (Figure 3). All Type 1 models exceeded 400 g at or before 4.7 m/s, which corresponds to a drop height of 1.22 m. Type 2 were under 200 g at 4.7 m/s and peaked at approximately 350 g. While Type 2 models did not exceed 400 g, they were not tested at the final height as they were already close to the threshold and expected to exceed it. Additionally, all Type 1 models reached a HIC value of 1500 at or before 4.7 m/s while the Type 2 models were below 1000 at this velocity. Type 2 models exceeded a HIC value of 1500 at 5.7 m/s and peaked at approximately 2500.

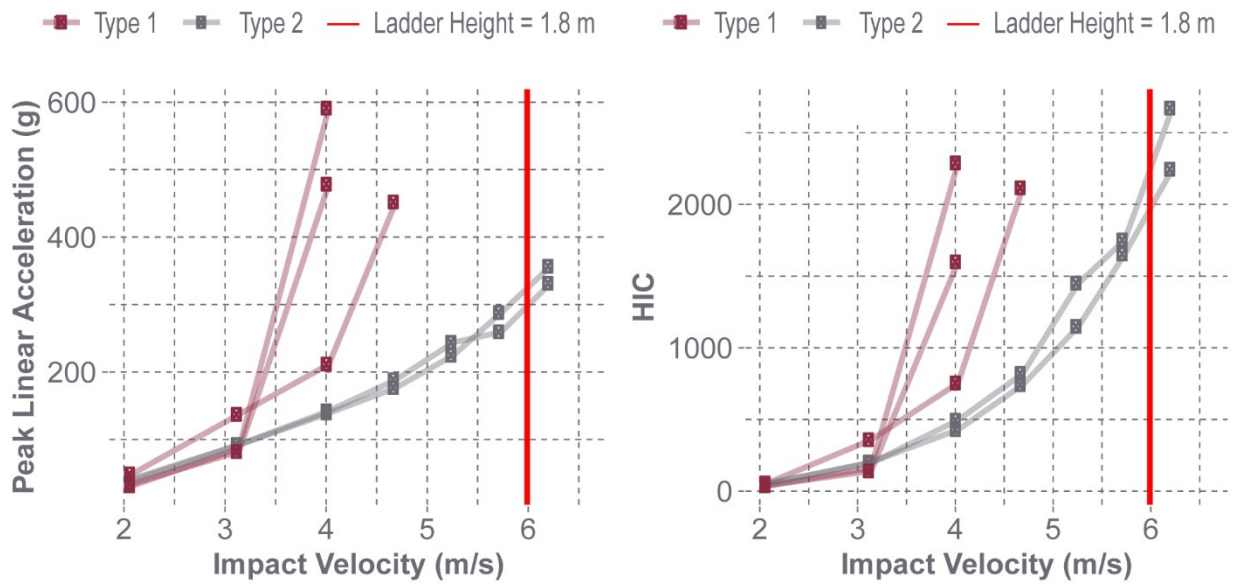


Figure 1.3 Peak linear acceleration (PLA) (g) and HIC 15ms for all hard hat models at the side impact location. Both PLA and HIC were lower for Type 2 hard hats compared to Type 1. “Ladder Height” corresponds to a theoretical velocity of 6.0 m/s and fall height of 1.8 m, which is the 25th percentile fall height from ladders. All 3 Type 1 models exceeded 400 g before 1.8 m.

Finally, for the oblique impact locations, Type 2 hard hats still had lower PLA and HIC values compared to Type 1 (Figure 4). Both types performed best at the oblique location. One Type 1 model exceeded 200 g before 4.7 m/s, while the other two Type 1 models did not exceed 200 g until after 5.3 m/s. The Type 2 models were under 200 g at 5.3 m/s and never exceeded 300 g. Similar results were observed for HIC. Two of the three Type 1 models reached a HIC value of approximately 1500 at 5.7 m/s while the other Type 1 model reached 1500 at 4.7 m/s. One Type 2 model exceeded a HIC value of 1500 at 6.6 m/s while the other Type 2 model peaked at approximately 1000.

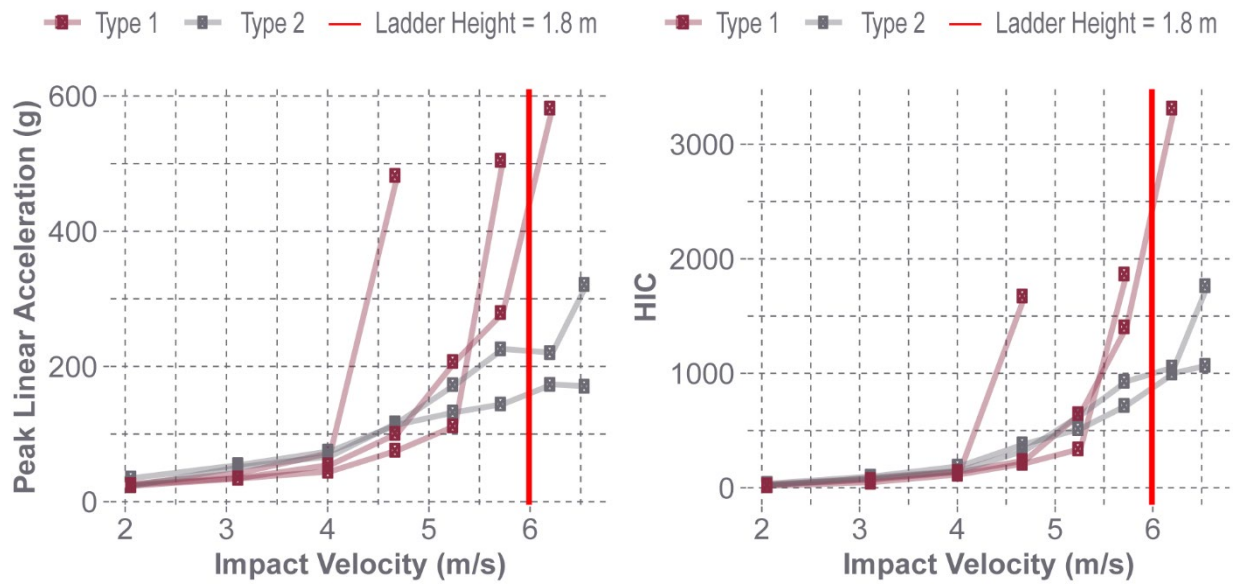


Figure 1.4 Peak linear acceleration (PLA) (g) and HIC 15ms for all hard hat models at the oblique impact location. Both PLA and HIC were lower for Type 2 hard hats compared to Type 1. “Ladder Height” corresponds to an impact velocity of 6.0 m/s and fall height of 1.8 m, which is the 25th percentile fall height from ladders. Two Type 1 models exceeded 400 g before 1.8 m.

Skull fracture risk when using Type 2 hard hats was substantially less than Type 1 hard hats for all three locations (Figure 5). Skull fracture risk for each type can be compared at 5.7 m/s, which corresponds to a fall height of 1.83 m and theoretical velocity of 6.0 m/s. This height is the 25th percentile fall height from ladders. At 5.7 m/s, Type 2 hard hats reduced skull fracture risk by approximately 64% (oblique), 92% (rear), and 34% (side) compared to Type 1. Differences in risk reduction were seen between locations. Both types performed the best at the oblique location and the worst at the side location. The greatest risk reductions between type were seen in the rear location.

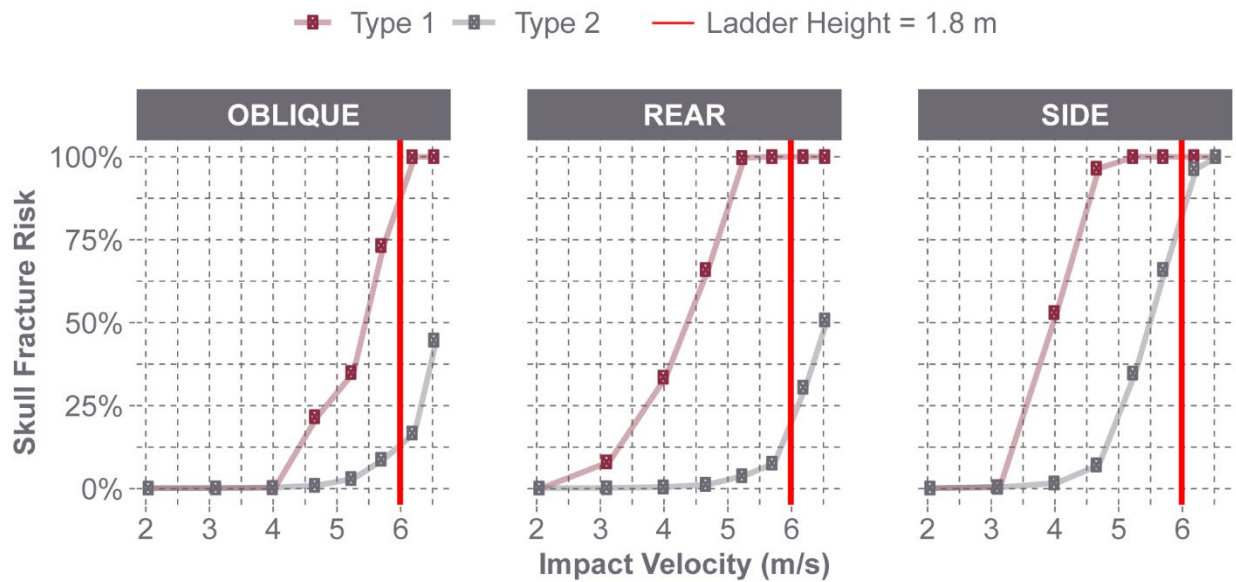


Figure 1.5 Skull fracture risk calculated from HIC as a function of impact velocity. Skull fracture risk was substantially less for Type 2 hard hats compared to Type 1, across all locations. “Ladder Height” corresponds to an impact velocity of 6.0 m/s and fall height of 1.8 m, which is the 25th percentile fall height from ladders. At this height, skull fracture risk was less for Type 2, and differences were seen between each location.

Similarly, concussion risk was less when using Type 2 hard hats rather than Type 1, for all three locations (Figure 6). At 5.7 m/s, Type 2 hard hats reduced concussion risk by 53% (oblique), 78% (rear), and 2% (side) compared to Type 1. Differences between locations were also seen. The oblique location had the best performances, the side had the worst performances, and the greatest differences between types seen in the rear location.

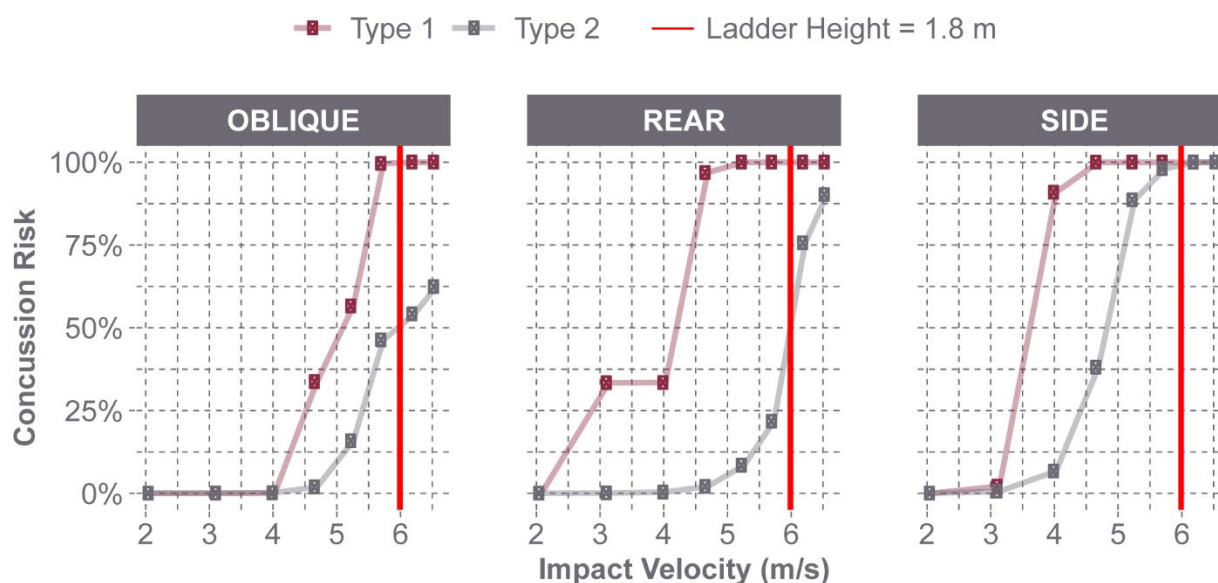


Figure 1.6 Concussion risk as a function of impact velocity. Concussion risk was less for Type 2 hard hats compared to Type 1, across all locations. “Ladder Height” corresponds to an impact velocity of 6.0 m/s and fall height of 1.8 m, which is the 25th percentile fall height from ladders. At this height, concussion risk was less for Type 2, and differences were seen between each location.

Discussion

This study's objective was to evaluate the ability of Type 1 and Type 2 hard hats to reduce head injury risk due to falling. The nature of construction accidents involving falls and the heights at which workers fall both varied. There is likely the most potential to reduce injuries and fatalities at low fall heights. A previous study conducted using OSHA data from January 1997 to October 2001 reported that 22.5% of all construction industry falls were between 0 m and 3.1 m (0 ft -10 ft) [9]. They also found head injuries accounted for approximately half of all fall injuries, but only 25% of all construction industry injuries [9]. Similarly, our study looked specifically at head injuries due to falls, and found that 31 of the 76 falls (41%) occurred at heights at or below 3.1 m (10 ft). This demonstrates that falls from low heights are responsible for a substantial portion of construction falls. It also highlights that these low fall heights are capable of producing a large

percentage (41%) of all the head injuries due to falls. This disproportionate rate of falls associated with head injuries emphasizes the need for improvements. Additionally, our study found that 22 of the 76 falls (29%) occurred at or below 2.4 m (theoretical velocity = 6.9 m/s). Of these 22 falls, 8 resulted in a skull fracture, including 1 fatality. We observed that Type 2 hard hats reduced skull fracture risk at 2.4 m by 55% for an oblique impact and 49% for a rear impact compared to Type 1 hard hats. For these fall types, Type 2 hard hats may be able to reduce future incidences of skull fracture.

Falls from ladders and scaffolds accounted for 46% of all falls. This finding is similar to values reported in the literature, which were between 23.2% and 40% [9-11]. At 1.83 m, the 25th percentile fall height for both ladders and scaffolds, Type 2 hard hats reduced skull fracture risk and concussion risk substantially compared to Type 1. The greatest reductions were seen in rear impacts, with skull fracture risk reduced by 92% and concussion risk reduced by 78%.

Current standards for hard hats set by the American National Standards Institute consider severe injury prevention and use linear acceleration thresholds to do so. Current standards determine that for Type 2 hard hats peak acceleration of the headform must be below 150 g for an impact velocity of 3.5 m/s. This velocity corresponds to a theoretical test height of 0.61 m (24"). These standards do not include acceleration criteria for impact attenuation performance of Type 1 hard hats. Testing in this study aimed to be consistent with current standards and used linear acceleration to determine injury risk. For the side location, none of the Type 1 models tested met the PLA requirements set by the Type 2 standards. One Type 1 model did not meet this requirement for the rear location. Additionally, the theoretical fall height from the standards is less than the heights provided in the construction accident reports, meaning real-world PLA values would tend

to be higher than the standard conditions. Skull fracture risk was shown to increase to 100% at a velocity of 5.3 m/s for both rear and side locations.

This study included three impact locations: rear, side, and oblique. These locations were assumed to be frequent head impact locations during a fall from height. While there is limited literature available on such injury scenarios, more research is needed to understand the biomechanics of typical falls, slips, and trips. When fall direction was analyzed as a function of disturbance type, it was reported that slips produced sideways or backwards falls for 72-79% of all slips, whereas trips most often led to forward falls (93-100%) [12]. Additionally, one study of construction accidents involving falls found that the immediate source of falls for one-third (911 out of 2,741) of the cases was due to the working surface [9]. These accidents included typical situations where workers slipped, such as workers that “slipped on the walking surface of the scaffolds and fell” [9]. These findings provide support toward using the selected locations, because workers are likely to fall backwards or sideways at these low heights.

Important distinctions in performance were seen between locations. Type 2 models performed better than Type 1 models across all locations, and the greatest risk reduction differences were seen at the rear location. The oblique location showed the best performance for all models regardless of the type, and the Type 1 performance was the most similar to Type 2 hard hats at this location. Type 2 performance was substantially worse at the side location. These location effects highlight inconsistencies in hard hat design, as well as the need to consider the hard hat as a system in which the shell, suspension, and foam liner all contribute to their performance. We suspect that the oblique location had the best performance because the higher elevation allowed the suspension system to be more effectively engaged. Type 2 hard hats likely performed the best at rear and oblique impacts because they engaged both the suspension system

and the foam liner. It can be further hypothesized that both types had the worst performances for side impacts because there were less time and space within the hard hat design for the suspension to be engaged. This resulted in the shell, and the foam liner for Type 2 models, becoming the main source of energy dissipation.

Differences in performance between location may be further distinguished due to outliers in the relationship between PLA and HIC at higher velocity impacts. For example, in the oblique and rear locations we see HIC values of approximately 2000 for Type 1 models despite PLA values over 400 g that would clearly indicate a severe injury. In these short-duration impacts that the hard hat “bottoms-out,” HIC may be under-detecting bottoming-out effects and under-estimating injury potential. While skull fracture risk based on HIC appeared to be a better predictor of injury than PLA for this study, and there is a lack of definitive data identifying HIC as a superior metric compared to PLA, this limitation of HIC must be considered.

This study was limited by the number of samples and impact locations used in testing. Hard hat models were grouped to represent each hard hat type, and a comparison of PLA and HIC values showed a wide variation in responses among Type 1 models. Type 1 standards appear to allow a wide range of responses to off-center impacts. Type 2 models showed better agreement in their responses. Furthermore, we assume that the individual falls head first rather than impacting their body first. In reality, the head impact velocity would be less than the velocity associated with the fall height, so the benefit of Type 2 hard hats might be greater than what we report. This would also alter the rotational accelerations experienced, which have not yet been effectively quantified for construction applications. Future work should look to better characterize the mechanics of how individuals fall from elevation. This would help to better represent linear head impact velocities and allow for rotational contributions to be quantified.

This study identified substantial variation in the ability of different hard hat types to reduce the risk of head injury due to falls in the construction industry. Inconsistencies in hard hat design were identified between models, types, and also between locations. Type 2 hard hats were shown to substantially reduce injury risk when compared to Type 1 hard hats. Results of this study suggest that Type 2 hard hats should be worn across all construction work. It also suggests that testing should be included in standards for both types that better represent real-world injury scenarios. Overall, these findings indicate that the risk of severe head injuries in the construction industry would be substantially reduced if more workers wore Type 2 hard hats.

Conclusion

The purpose of this study was to compare fall-related head injury risks for Type 1 and Type 2 construction hard hats. Three impact locations, rear, side, and oblique, were evaluated over a range of low fall heights. Type 2 models had lower PLA and HIC values. Type 2 hard hats substantially reduce skull fracture and concussion risk, for all impact locations, when compared to Type 1 hard hats. These findings indicate that the risk of severe head injuries in the construction industry would be substantially reduced if more workers wore Type 2 hard hats.

References

- [1] H. M. Tiesman, S. Konda, and J. L. Bell, "The epidemiology of fatal occupational traumatic brain injury in the US," *American journal of preventive medicine*, vol. 41, no. 1, pp. 61-67, 2011.
- [2] CPWR, *The Construction Chart Book: The U.S. Construction Industry and Its Workers*, X. S. Dong, ed., 6th ed. Silver Springs, MD: CPWR- The Center for Construction Research and Training, 2018.
- [3] G. M. Waehrer, X. S. Dong, T. Miller, E. Haile, and Y. Men, "Costs of occupational injuries in construction in the United States," *Accident Analysis & Prevention*, vol. 39, no. 6, pp. 1258-1266, 2007.
- [4] *American National Standards for Industrial Head Protection, ANSI/ISEA Z89.1-2014 (R2019)*, I. American National Standards Institute, Arlington, VA 22, 2014.
- [5] H. J. Mertz, P. Prasad, and G. Nusholtz, "Head injury risk assessment for forehead impacts," SAE Technical Paper, 0148-7191, 1996.
- [6] H. Mertz, P. Prasad, and G. Nusholtz, "Head Injury Risk Assessments Based on 15 ms HIC and Peak Head Acceleration Criteria," *NASA*, no. 19980003889, 1997.
- [7] P. Prasad and H. J. Mertz, "The position of the United States delegation to the ISO Working Group 6 on the use of HIC in the automotive environment," *SAE transactions*, pp. 106-116, 1985.
- [8] S. Rowson and S. M. Duma, "Development of the STAR evaluation system for football helmets: integrating player head impact exposure and risk of concussion," *Annals of biomedical engineering*, vol. 39, no. 8, pp. 2130-2140, 2011.
- [9] X. Huang and J. Hinze, "Analysis of construction worker fall accidents," *Journal of construction engineering and management*, vol. 129, no. 3, pp. 262-271, 2003.
- [10] G. Mistikoglu, I. H. Gerek, E. Erdis, P. M. Usmen, H. Cakan, and E. E. Kazan, "Decision tree analysis of construction fall accidents involving roofers," *Expert Systems with Applications*, vol. 42, no. 4, pp. 2256-2263, 2015.
- [11] E. A. Nadhim, C. Hon, B. Xia, I. Stewart, and D. Fang, "Falls from height in the construction industry: a critical review of the scientific literature," *International journal of environmental research and public health*, vol. 13, no. 7, p. 638, 2016.
- [12] W. C. Hayes, M. S. Erickson, and E. D. Power, "Forensic injury biomechanics," *Annu. Rev. Biomed. Eng.*, vol. 9, pp. 55-86, 2007.

CHAPTER 2

Comparison of Head Impact Events in Motorsport Simulations and Laboratory Tests

Abstract

Professional motorsports, such as the National Association of Stock Car Racing (NASCAR), attract many fans because of its high-speed excitement, but these high speeds also make it an inherently high-risk occupation for professional racers. Despite a history of serious injuries, NASCAR has made many improvements to safety standards within the last 20 years. The risk of fatalities and severe injury has greatly decreased, but head injury remains a concern. NASCAR helmets must meet a set of performance standards, which include impact attenuation, penetration, and fire resistance criteria. Modifications to racing helmets, such as communication systems, and visors, are sometimes added to assist drivers. However, these modifications are not overseen by any regulatory bodies and have the potential to alter helmet performance. Therefore, the purpose of this study was to compare simulation data to laboratory tests intended to simulate motorsport head impact events. This will eventually support the development of an experimental protocol for evaluating motorsport head impact events and the effects of helmet modifications on helmet integrity and head injury risk.

Simulation data representing real-world NASCAR collisions were modeled and processed at Wake Forest University for a 50th percentile male. Collision kinematics, including change in velocity (ΔV) for the car and head, and principal direction of force (DOF) were provided for 45 impacts and were used to inform experimental tests. A pneumatic ram impactor and instrumented 50th percentile Hybrid III headform and neck were used for laboratory tests. Ten helmet locations, corresponding to ten selected DOFs, were tested using five HJC motorsport helmets. Each helmet was used for two locations, and each location was tested at five impact

velocities to encompass a functional helmet performance range: 2.0 m/s, 3.0 m/s, 4.0 m/s, 5.0 m/s, and 6.0 m/s. The headform was instrumented with a 9-accelerometer array and triaxial rate sensor. The impactor ram had a 5.5 kg steel plate attached and instrumented with an accelerometer, with a 1” thick piece of head surround foam (EIS W18, BSCI, Mooresville, NC) added on top of the plate. Peak acceleration, delta V, and deformation were calculated for each test and compared to the simulation results. Deformation and delta V were used as measures of impact energy and allowed comparison of the isolated head impact event in the laboratory tests and simulations.

Simulation deformations were generally less than the lab deformations, while delta V was aligned well with the lab results. Regression analyses were used to create relationships between the lab deformation and acceleration and the lab delta V and acceleration. They were then used to estimate lab kinematics using simulation specified deformation and delta V values. The deformation-based model performed better for frontal DOF conditions, while the delta V-based model performed better for rear and side DOF conditions. Overall, laboratory tests are typically completed at high severities greater than typical crashes. The real-world simulation results typically had lower kinematics but were likely involving higher energy levels that were managed by surrounding protective systems. These findings can be used to inform future helmet testing protocols to better represent real-world impacts.

Introduction

Motorsports are popular sports that attract both amateur and professional competitors and millions of fans. There are many different types of professional motorsports and sanctioning companies, but the National Association of Stock Car Racing (NASCAR) is one of the most popular. NASCAR attracts many fans because of its high-speed excitement, but these high speeds also make it an inherently high-risk occupation for professional racers.

In the last 20 years, there have been efforts to improve motorsport safety following some high-profile fatalities within the sport [1]. These fatalities revealed that the high-velocity crashes produced high forces on the neck that led to catastrophic craniovertebral junction injuries [1]. In response, the Head and Neck Support (HANS) device was developed to reduce neck loading and head acceleration, and was soon required by NASCAR and other racing regulatory bodies [1]. There have since been several other safety improvements made, including the SAFER (Steel And Foam Energy Reduction) barrier, restraint system requirements, and energy-absorbing head impact padding [2]. Standards for these improvements are regulated by NASCAR, SFI Foundation (SFI), FIA, and Snell Foundation, which all establish motorsport equipment safety standards [3-6]. Computational modeling techniques have also been used to model crashes and predict injury risk [7].

While these changes have substantially improved professional racer safety, there are still many concerns around head injuries in the sport. Severe head injury rates have decreased, but concussion rates are poorly defined and appear high [8, 9]. Surveying medical professionals and racers indicates that concussions are common within the sport [10]. Issues of under-reporting injuries and multiple concussions were also a concern and could increase risk for long-term consequences [10]. Helmets and other safety measures will never eliminate head injury risk, but

improvements can reduce risks and severity. NASCAR requires helmets to meet standards established by one of several regulatory bodies: Snell Foundation, SFI Foundation, FIA. These standards specify a series of tests for impact attenuation, penetration resistance, and fire resistance, among other things [3, 5].

However, improvements in technology and efforts to be competitive in the sport have led racing teams to modify helmets with small cameras, headsets, and visors. This trend has been seen in other sports such as cycling [11], but these modifications are not covered within helmet regulatory guidelines, and the effects that these changes may cause on helmet integrity are unknown. Additionally, many racing safety standards are performed using instrumented test sleds, which are expensive and time-intensive. The ability to evaluate the effects of these modifications on a component-level test rig would be beneficial to NASCAR, motorsports safety foundations, and manufacturers.

Therefore, the purpose of this study was to compare simulation data to laboratory tests intended to simulate motorsport head impact events. Simulations will be used to inform experimental tests and isolate head impact events in the laboratory, and results will be compared between full collision scenarios and component-level laboratory tests. This will eventually support the development of an experimental protocol for evaluating motorsport head impact events and the effects of helmet modifications on helmet integrity and head injury risk.

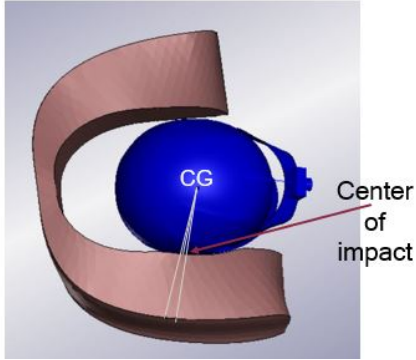
Methods

The objective of this study was to compare simulation data to laboratory tests intended to simulate motorsport head impact events. Simulations informed experimental tests, and head impact events were isolated to compare the energy involved. The overall steps and rationale used are provided in the list below. Table 2.1 provides a comparison of the simulation and laboratory setups.

1. Simulation data representing real-world NASCAR collisions were modeled and processed at Wake Forest University for a 50th percentile male. Collision kinematics, including change in velocity (ΔV) for the car and head, and principal direction of force (DOF), were provided for 45 impacts.
2. Simulations were used to inform laboratory impact tests using a pneumatic ram impactor and instrumented 50th percentile Hybrid III headform and neck. 10 helmet locations, corresponding to 10 DOFs, were tested using 5 HJC motorsport helmets. Each helmet was used for two well-spaced locations. Each location was impacted at five impact velocities (2.0 m/s, 3.0 m/s, 4.0 m/s, 5.0 m/s, and 6.0 m/s) to test a range of impact energies and allow a regression-based comparison of the laboratory tests and simulations.
3. In order to compare the isolated head impact events in the laboratory with the head impacts within the much longer duration full collision simulations, energy levels were compared, using ΔV and deformation. These values were used to understand the energy managed by the helmet versus transferred to the head. Associated accelerations for these impacts were also compared.
 - a. Peak linear acceleration (PLA), ΔV , and total deformation were calculated from the laboratory tests.

- b. The same metrics, PLA, delta V, and deformation, were calculated from the simulations. Deformation of the helmet, head surround, and combined total deformation, were all considered from the simulations.
4. Regression analyses established relationships between deformation and acceleration as well as delta V and acceleration, for the laboratory results. These relationships were then used to estimate lab kinematics at simulation specified deformations and change in velocities.

Table 2.1 Comparison of the simulation and laboratory setups. Simulations were used to inform laboratory testing. An exact comparison was not needed, but rather a comparison of the energy managed within the isolated head impact event for both.

	Simulations	Laboratory Setup
		
Component Level	Full crash scenario	Isolated head impact event
Test Rig	Full-sled crash simulation	Pneumatic linear impactor with rigid steel impactor face
Helmet	General helmet model	five HJC H10 helmets (HJC Motorsports, La Habra, CA)
Headform/Model	50 th percentile male simplified occupant model (M50-OS) from the Global Human Body Models Consortium (GHBMC)	Instrumented 50th percentile male Hybrid III headform and neck
Impact Surface	Full head surround	5.5 kg rigid steel impactor face with 1” thick head surround foam attached
Padding Properties	head surround foam, properties closely matched with lab (EIS W18, BSCI, Mooresville, NC)	1” thick piece of head surround foam (EIS W18, BSCI, Mooresville, NC)
Impact Locations	Determined as contact point between helmet and head surround	Estimated from impact locations on simulation helmet
Initial Positions	Head and neck positions estimated using simulation measurement tools	Head and neck positions set using simulation estimates
Impact Velocities	Change in velocity measured for duration of contact	Range of velocities tested to capture velocities seen in simulations
Deformations Measured	Helmet, head surround, computed and measured total for the system	Total for the system (helmet and impactor padding)

Simulation Data Reduction

Simulation data representing real-world NASCAR collisions were modeled by Wake Forest University using a 50th percentile male simplified occupant model (M50-OS) from the Global Human Body Models Consortium (GHBMC) integrated into a NASCAR motorsport environment [12]. This biofidelic computational model is used to assess occupant safety in pedestrian vehicles and is comparable to the average NASCAR driver and Hybrid III anthropometric testing device (ATD) [12]. These data included 45 impact scenarios which informed the development of a laboratory testing procedure. Latitudinal and longitudinal delta V were provided. Resultant delta V and DOF were calculated from this information. For this analysis, we only considered the 50th percentile male condition.

A number of steps were taken to reduce the data set further and establish representative impact angles and speeds. First, generalized angles were set as 1-degree increments between 0° and 360°. The difference between the DOF of each impact and each generalized angle value was calculated, resulting in a list of 361 differences for each impact simulation. The two impacts with the smallest difference in direction from the generalized value were recorded for each generalized angle. The average difference and the difference between the two difference values were calculated for each generalized angle as a measure of variance. The absolute change in velocity between the two impacts was also calculated as an indication of their spread in magnitude. This resulted in eight metrics for each of the generalized angles which were used in reducing the data set.

First, all generalized values that had a second difference greater than 2° were removed. A 2° threshold was selected because it effectively reduced the data set while still maintaining the impact distribution shape. Next, duplicates were removed by identifying the cases of duplicate change in velocity magnitudes and removing the case with the greater difference between impact

1 and impact 2 differences. This resulted in 29 generalized angle value options. From these 29 options, angles were incrementally removed if the next angle was less than 5° from the angle before it. This resulted in 16 options. Adjustments to this threshold value and offset resulted in minimal differences in the angles selected. Finally, any cases in which the change in velocity between the two impacts was greater than or equal to 60 kph (16.67 m/s) were removed based on limitations of typical laboratory testing equipment. This resulted in a final data set of 12 angles and 24 impacts, two impacts per angle. The impact locations were as followed, in degrees, where 0° is a purely frontal crash, positive values are in a clockwise direction, and negative values are in a counterclockwise direction: 2°, 9°, 15°, 21°, 37°, 54°, 70°, 75°, -74°, -55°, -21°, -9°. The head is symmetric about the midsagittal plane, but the car interior structure is not. For this reason, symmetry was not assumed and mirrored locations (21° and -21°, 9° and -9°) were tested separately.

Laboratory Testing Methods

Simulation post-processing files (LS-PrePost, Livermore Software Technology Company (LSTC), Livermore, CA) were used to visualize the impact between the helmet and head surround foam. Specifically, initial head and neck positions were approximated. Neck angles were evaluated using measurement tools between the head form center of gravity (CG) and multiple neck components. helmet impact location was identified visually using a Von Mises Stress map to find the region of initial impact. Impact scenarios were combined for the 70° and 75° impacts, as well as the 2° and 9° impacts, because their helmet centers of impact closely overlapped. This resulted in 4 left side impacts (DOF: -9°, -21°, -55°, -74°) and 6 right side impacts (DOF: 9°, 15°, 21°, 37°, 54°, 75°) for laboratory testing. Impact locations can be seen in Figure 2.1. Locations ranged from rear boss, center of the side of the helmet, and lower front side. Locations will be summarized as Conditions A-J in the following order: 75°, 54°, 37°, 21°, 15°, 9°, -9°, -21°, -55°, and -74°. Head

kinematics provided for each simulation impact were used to calculate peak linear acceleration (PLA) and were considered when selecting laboratory testing conditions.

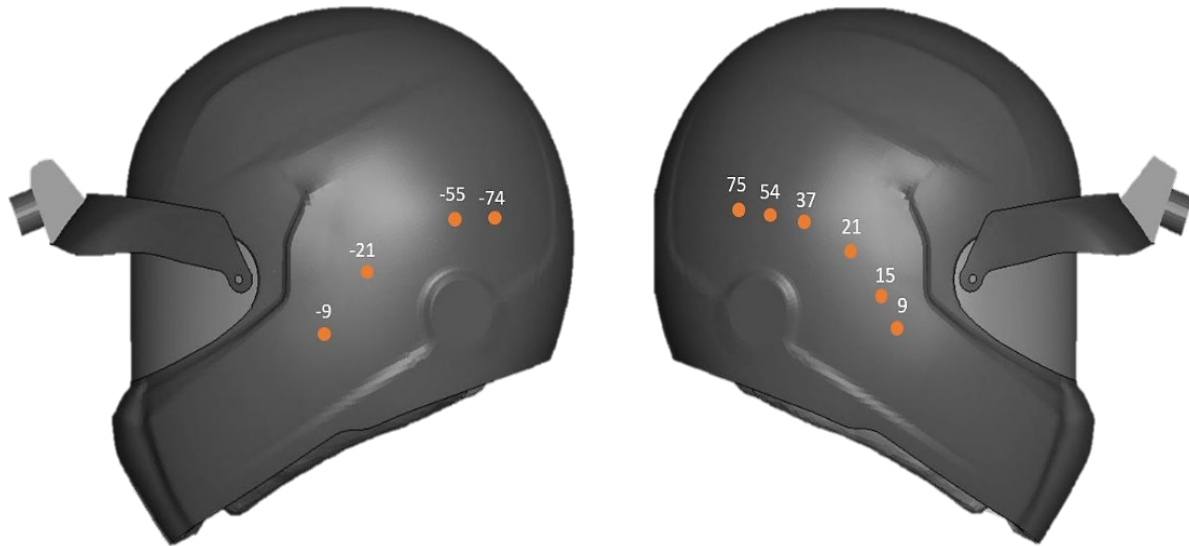


Figure 2.1 Overview of left side (left) and right side (right) impact locations tested. Locations are labeled according to the corresponding simulation DOF. There are four left side impacts (DOF: -9°, -21°, -55°, -74°) and six right side impacts (DOF: 9°, 15°, 21°, 37°, 54°, 75°).

A pneumatic linear impactor was used to test ten impact locations. A 50th percentile male Hybrid III headform and neck were mounted on a 16-kg linear sliding table with 5 degrees of freedom (Biokinetics, Ottawa, Canada). The sliding table was adjusted for each impact location according to the head and neck positions identified in the simulations. The headform was instrumented with a 9-accelerometer array (Endevco 7264B-2000, Meggitt Sensing Systems, Irvine, CA) and triaxial angular rate sensor (ARS3 PRO-18K, DTS, Seal Beach, CA) according to SAE J211 specifications. Preliminary tests were completed to establish the pressure-velocity relationship of the pneumatic ram. Impact velocities were chosen in order to test a range of impact energies that would allow the development of linear relationships and estimation of simulation based equivalent values. The selected impactor velocities were 2 m/s, 3 m/s, 4 m/s, 5 m/s, and 6

m/s. The impactor end of the ram was outfitted with a 5.5 kg steel plate. An accelerometer was placed within the center of the steel plate in order to measure impactor acceleration in the x-direction. A 1” thick piece of head surround foam (EIS W18, BSCI, Mooresville, NC) was cut to fit the steel plate and secured to the end of the ram.

Ten impact locations were tested between five HJC H10 helmets (HJC Motorsports, La Habra, CA). Each helmet was tested for two locations. Locations were assigned such that impact centers were a minimum of 140 mm apart to avoid overlapping damage, as specified by standards set by the Snell Foundation [3]. The same helmet was impacted for all five impact velocities.

Simulation Deformation Analysis

Deformation and delta V values were calculated from the simulations as energy correlates of the head impact. Deformation was measured using simulation post-processing files (D3plots, LS-PrePost, LSDYNA). Deformation for the helmet, head surround, and total deformation were measured for each of the 24 impacts. Total deformation was also computed from the helmet and head surround components. The head delta V was calculated for each simulation impact from the provided kinematics, using the same time frame as the deformation calculations. PLA, peak rotational velocity (PRV), and Head Injury Criterion (HIC) 15 ms, were also calculated from the provided simulation kinematics.

In order to measure deformations, the x, y, z components, and the resultant distance, were measured between a “node” of interest and the head CG within the simulation files. Deformation was calculated as the change in resultant distance between the node and head CG, from the point of initial contact until the minimum distance. Initial contact was determined when the resultant distance noticeably decreased in value. Duration was determined as one time frame before the decrease in distance was observed until the time frame at which minimum distance was reached.

For the helmet deformation, the node of interest was placed at the center of impact on the helmet. Center of impact was found using a Von Mises Stress map and by visual inspection of contact between the helmet and head surround. For the head surround, two nodes of interest were selected on the outer edge of the surround. Two points were used to account for movement of the helmet along the head surround during impact. These points experienced maximum deformation at approximately the same time frame as the helmet maximum deformation and were positioned as boundaries around the helmet node movement. Total measured deformation was calculated between each surround point and the head CG, and an average was calculated. Head surround deformation was calculated between each surround point and the helmet node, and the average was calculated. Finally, computed totals were calculated by adding the helmet and surround components for each surround point and determining two new resultants. From here, an average resultant distance was calculated and computed total deformation was found.

Laboratory Deformation Analysis

Deformation and delta V were calculated for the laboratory results as energy correlates for the head impact. PLA, PRV and HIC 15 ms were also calculated for the laboratory results. A number of steps were taken to do so. First, SAE J211 low pass filters were used to filter the acceleration data using Channel Frequency Class (CFC) 1000 and angular rate data using CFC 155. Maximum resultant acceleration was calculated from the x, y, and z accelerometers at the head CG. Then, head CG acceleration and angular rate data were rotated to align with the laboratory global coordinate system. The angles about the y-axis and z-axis, determined when setting the laboratory initial headform positions, were used in the rotation matrix for each corresponding location. Angle changes were then calculated for each time step by integrating the angular rate data. These angle changes were used in another rotation matrix, in which the angle

change was applied at each time step, in order to rotate the acceleration data back to the global coordinate system at each time step.

Once all data was rotated to the global system, velocities and displacements were calculated for the head CG and impactor. Velocity was calculated by integrating acceleration data for all components. Delta V was found by taking the difference between the maximum resultant velocity and the resultant velocity at the first time point. Displacement was calculated by integrating the velocity data for all components. For each location, initial distances were recorded from the corresponding simulations as the x, y, and z components of the vector between the head CG and center of impact on the outer surface of the helmet. These initial distances were transformed to global coordinates, using the same initial rotation matrix. Then, they were set as laboratory initial positions, between the center of impact and head CG, where the center of impact on the helmet was the origin. These initial distances were added to the displacement data. Relative displacement was calculated by subtracting the impactor displacement data, which was constrained to the x-axis, from the CG x-displacement data. Finally, resultant relative displacement was calculated, and max deformation was found by subtracting the minimum resultant displacement from the resultant displacement at the first time point.

Regression Analysis and Predicted Accelerations

For each of the ten DOF conditions, two linear regression analyses were completed using the laboratory testing results. First acceleration as a function of deformation was analyzed, then acceleration as a function of delta V. In both cases, the model was constrained through zero. These relationships were then used to estimate lab kinematics at simulation specified deformations and change in velocities. The percent error between the predicted acceleration and simulation acceleration was found for both models. The use of linear regressions allows for interpolation

between the lab-tested impact conditions and representation of a range of potential real-world crash conditions.

Results

The results are summarized as Conditions A-J, which correspond to the simulation impact DOF values, in the following order: 75°, 54°, 37°, 21°, 15°, 9°, -9°, -21°, -55°, and -74°. Each condition presents simulation data, laboratory data, and the regression analysis results. Simulation data includes head delta V, head PLA, and deformation values for the helmet, head surround, computed total, and measured total. Laboratory data includes impactor velocity, headform delta V, headform PLA, and deformation. The regression analysis results provide predicted acceleration results and percent errors, for both regression models. For a complete summary table of the simulation results please see Table A.1 in Appendix A, and for a summary table of all laboratory results please see Table A.2 in Appendix A.

Condition A

The DOF was approximated as 75°. This resulted in an impact to the right rear boss region of the helmet.

Simulation and Laboratory Results

Four simulations were selected to represent this condition. The corresponding DOF values were: 69.3°, 76.7°, 71.5°, 73.2°. The car resultant delta V for these simulated impacts were: 23.8, 25.0, 12.5, 24.6 m/s. Table 2.2.a summarizes the simulation results for this condition, while the laboratory results can be seen in Table 2.2.b. Simulation deformations were less than lab deformations. Simulation delta V values (1.65 - 2.29 m/s) aligned well with the lower lab values (1.66 m/s and 2.85 m/s).

Table 2.2.a Simulation results for the 75-degree impacts. Helmet, head surround, computed total, and measured total deformations were all reported. Head delta V and head PLA were also determined.

Car Impact DOF (°)	Delta V (m/s)	PLA (g)	Deformation (mm)			
			Helmet	Head Surround	Computed Total	Measured Total
70	1.85	46.8	1.21	5.37	6.79	6.80
75	2.29	42.9	1.50	6.61	8.34	8.35
70	1.65	27.9	1.03	4.69	5.92	5.93
75	2.09	43.8	1.38	8.07	9.55	9.56

Table 2.2.b Laboratory results for the 75-degree impacts. Total deformation was recorded, as well as impactor velocity, headform delta V, and headform PLA.

Car Impact DOF (°)	Impactor Velocity (m/s)	Delta V (m/s)	PLA (g)	Deformation (mm)
75	1.98	1.66	22.8	14.9
75	3.16	2.85	56.6	19.3
75	3.98	3.70	95.0	21.8
75	5.05	4.81	91.1	27.6
75	6.12	5.72	127.8	30.3

Regression Analysis Results

Regression analysis results for the 75-degree impacts are shown in Table 2.2.c. Acceleration was underpredicted when deformation was the predictor variable. Predicted acceleration agreed well with simulation results when delta V was the predictor variable (average error: $6.8 \pm 17.8\%$). Figure 2.2 shows acceleration as a function of deformation and acceleration as a function of delta V. Both regression models fit the lab data well. The delta V-based model was a better predictor, with the estimated accelerations within the same range as the simulation results and lower range of the lab values.

Table 2.2.c Regression analysis results for the 75-degree impacts. Simulation and predicted accelerations are shown, with percent errors.

	Simulation PLA (g)	Acceleration as a Function of Deformation		Acceleration as a Function of Delta V	
		Predicted PLA (g)	Percent Error (%)	Predicted PLA (g)	Percent Error (%)
	46.8	24.5	-47.7	39.6	-15.3
	42.9	30.0	-30.0	49.0	14.2
	27.9	21.3	-23.5	35.2	26.4
	43.8	34.4	-21.4	44.7	2.0
Average			-30.7 ± 11.9		6.8 ± 17.8

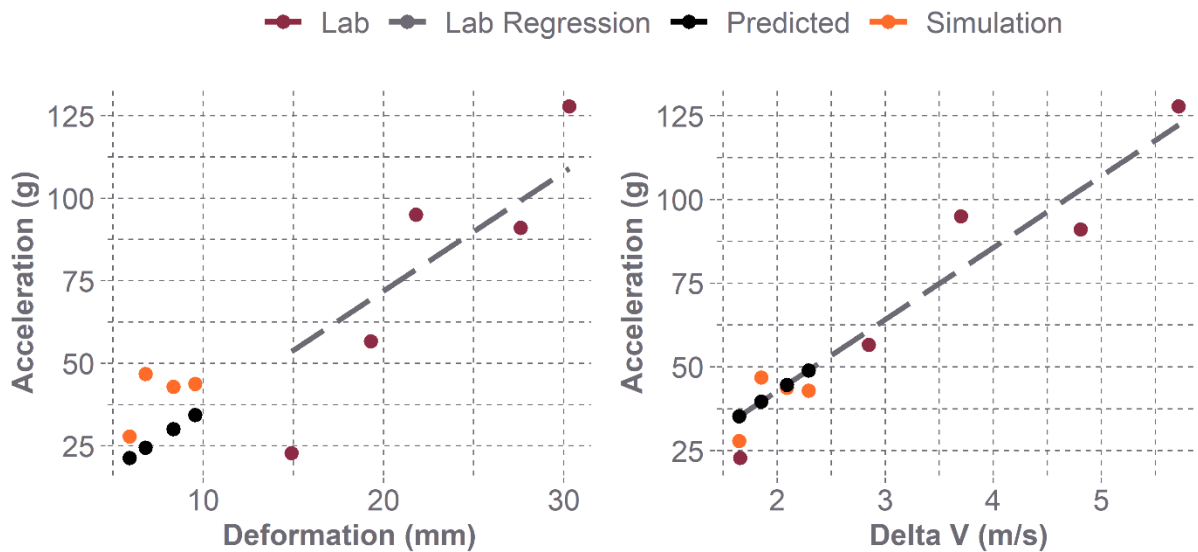


Figure 2.2 Acceleration as a function of deformation (left) and as a function of delta V (right) for the 75-degree impact condition. Both regression models fit the lab data well. The delta V-based model was a better predictor, with the estimated accelerations within the same range as the simulation results and lower range of the lab values.

Condition B

The DOF was approximated as 54°. This resulted in an impact to the right rear boss region of the helmet. This location was slightly farther forward and lower than the 75-degree impact.

Simulation and Laboratory Results

Two simulations were selected to represent this condition. The corresponding DOF values were: 53.4° and 54.7°. The car resultant delta V for these simulated impacts were: 17.3 and 26.3 m/s. Table 2.3.a summarizes the simulation results for this condition. The laboratory testing results can be seen in Table 2.3.b. Simulation total deformations values were less than the lab values, while delta V results (1.14 m/s and 1.51 m/s) were close to the lowest lab result (1.39 m/s).

Table 2.3.a Simulation results for the 54-degree impacts. Helmet, head surround, computed total, and measured total deformations were all reported. Head delta V and head PLA were also determined.

Car Impact DOF (°)	Delta V (m/s)	PLA (g)	Deformation (mm)			
			Helmet	Head Surround	Computed Total	Measured Total
54	1.14	37.1	1.08	3.52	4.85	4.85
54	1.51	67.0	1.20	4.72	6.22	6.22

Table 2.3.b The laboratory testing results for the 54-degree impacts. Total deformation was recorded, as well as impactor velocity, headform delta V, and headform PLA.

Car Impact DOF (°)	Impactor Velocity (m/s)	Delta V (m/s)	PLA (g)	Deformation (mm)
54	1.78	1.39	29.4	17.8
54	2.57	2.24	42.3	21.5
54	3.75	3.43	56.3	23.4
54	4.95	4.73	118.1	29.2
54	6.08	5.50	117.8	30.1

Regression Analysis Results

Regression analysis results for the 54-degree impacts are shown in Table 2.3.c. Both regression models underpredicted acceleration, but the delta V-based model had less error (-42.6%) than the deformation-based model (-64.7%). Figure 2.3 shows acceleration as a function of deformation and acceleration as a function of delta V. The delta V-based model was a better fit for the lab results. It was also a better predictor, with less error between the simulation and predicted accelerations.

Table 2.3.c Regression analysis results for the 54-degree impacts. Simulation, and predicted accelerations are shown, with percent errors.

	Simulation PLA (g)	Acceleration as a Function of Deformation		Acceleration as a Function of Delta V	
		Predicted PLA (g)	Percent Error (%)	Predicted PLA (g)	Percent Error (%)
	37.1	15.3	-58.7	24.6	-33.7
	67.0	19.7	-70.7	32.4	-51.6
Average			-64.7		-42.6

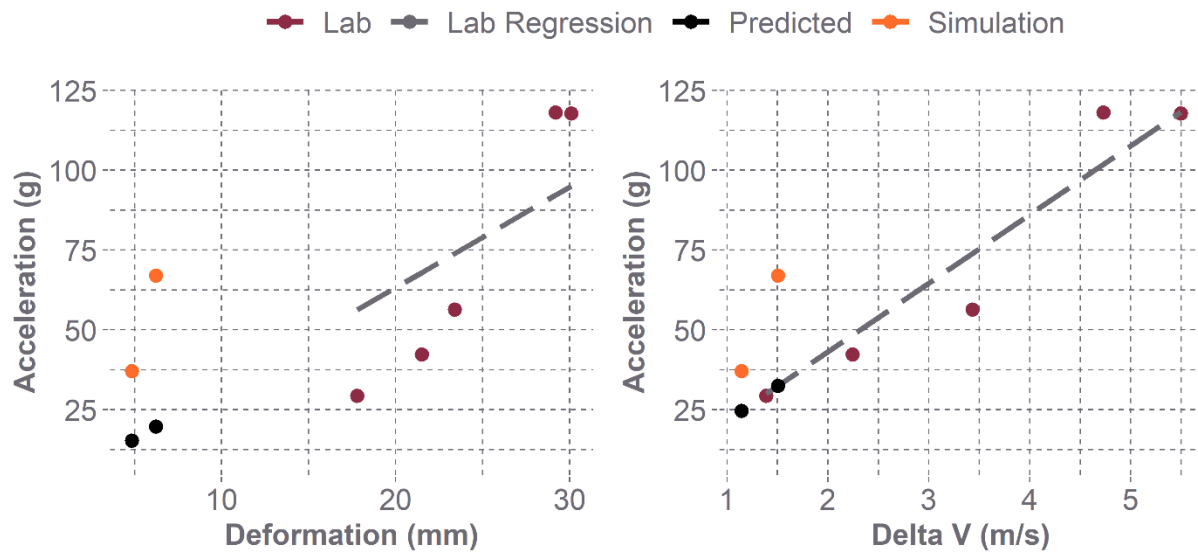


Figure 2.3 Acceleration as a function of deformation (left) and as a function of delta V (right) for the 54-degree impact condition. The delta V-based model was a better fit for the lab results. It was also a better predictor, with less error between the simulation and predicted accelerations.

Condition C

The DOF was approximated as 37°. This resulted in an impact to the center of the right side of the helmet.

Simulation and Laboratory Results

The DOF was approximated as 37°. The corresponding DOF values were: 37.4° and 36.0°. The car resultant delta V for these simulated impacts were: 22.1 m/s and 19.9 m/s. Table 2.4.a summarizes the simulation results for this condition. The laboratory testing results can be seen in Table 2.4.b. Simulation total deformations and delta V values were both much less than the lab results.

Table 2.4.a Simulation results for the 37-degree impacts. Helmet, head surround, computed total, and measured total deformations were all reported. Head delta V and head PLA were also determined.

Car Impact DOF (°)	Delta V (m/s)	PLA (g)	Deformation (mm)			
			Helmet	Head Surround	Computed Total	Measured Total
37	0.52	52.2	1.13	3.45	4.57	4.58
37	0.69	49.0	1.12	2.29	3.52	3.52

Table 2.4.b The laboratory testing results for the 37-degree impacts. Total deformation was recorded, as well as impactor velocity, headform delta V, and headform PLA.

Car Impact DOF (°)	Impactor Velocity (m/s)	Delta V (m/s)	PLA (g)	Deformation (mm)
37	2.00	1.74	26.0	16.5
37	3.18	2.93	45.1	19.7
37	4.05	3.71	67.1	23.1
37	5.08	4.70	94.7	27.0
37	6.08	5.47	114.0	32.3

Regression Analysis Results

Regression analysis results for the 37-degree impacts are shown in Table 2.4.c. Both regression models underpredicted acceleration substantially and had similar percent errors of -75.5% (deformation model) and -76.8% (delta V model). Figure 2.4 shows acceleration as a function of deformation and acceleration as a function of delta V. Both models underpredicted acceleration, but the delta V-based model was a better fit for the lab results, compared to the deformation-based model.

Table 2.4.c Regression analysis results for the 37-degree impacts. Simulation and predicted accelerations are shown, with percent errors.

	Simulation PLA (g)	Acceleration as a Function of Deformation		Acceleration as a Function of Delta V	
		Predicted PLA (g)	Percent Error (%)	Predicted PLA (g)	Percent Error (%)
	52.2	14.1	-73.1	10.1	-80.7
	49.0	10.8	-78.0	13.3	-72.9
Average			-75.5		-76.8

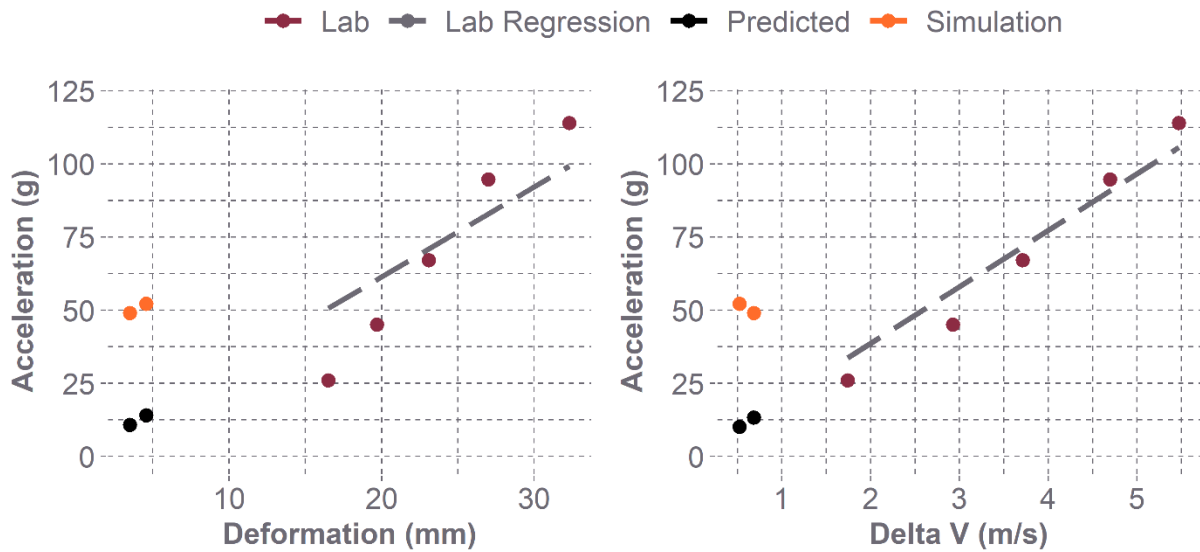


Figure 2.4 Acceleration as a function of deformation (left) and as a function of delta V (right) for the 37-degree impact condition. Both models underpredicted acceleration, but acceleration as a function of delta V fit the lab data better.

Condition D

The DOF was approximated as 21°. This resulted in an impact to the center of the right side of the helmet, slightly in front of the 37-degree condition.

Simulation and Laboratory Results

Two simulations were identified to represent the 21° car impact condition. The DOF values were: 20.1° and 22.9 °. The car resultant delta V for these simulated impacts were: 23.5 m/s and 7.1 m/s. Table 2.5.a summarizes the simulation results for this condition. The laboratory testing results can be seen in Table 2.5.b. Simulation total deformations (5.93 mm, 7.14 mm) were less than the smallest lab deformations (14.9 mm), but delta V values were more aligned.

Table 2.5.a Simulation results for the 21-degree impacts. Helmet, head surround, computed total, and measured total deformations were all reported. Head delta V and head PLA were also determined.

Car Impact DOF (°)	Delta V (m/s)	PLA (g)	Deformation (mm)			
			Helmet	Head Surround	Computed Total	Measured Total
21	4.61	62.0	2.10	5.37	5.92	5.93
21	0.86	31.1	1.52	6.18	7.13	7.14

Table 2.5.b The laboratory testing results for the 21-degree impacts. Total deformation was recorded, as well as impactor velocity, headform delta V, and headform PLA.

Car Impact DOF (°)	Impactor Velocity (m/s)	Delta V (m/s)	PLA (g)	Deformation (mm)
21	1.80	1.53	22.9	14.9
21	3.17	2.87	53.8	19.8
21	4.00	3.65	70.9	23.1
21	4.90	4.55	81.3	28.9
21	6.16	5.72	119.4	32.8

Regression Analysis Results

Regression analysis results for the 21-degree impacts are shown in Table 2.5.c. When deformation was the predictor variable, acceleration was underpredicted. When delta V was the predictor variable, the predicted accelerations (89.5 g and 16.7 g) fell above and below the simulation values (62.0 g and 31.1 g), and had an average percent error of -1.0%. Figure 2.5 shows acceleration as a function of deformation and acceleration as a function of delta V. Both regression models fit the lab results well, with the delta V-based model fitting slightly better. The delta V-based model was a better predictor of accelerations, with a very low average error.

Table 2.5.c Regression analysis results for the 21-degree impacts. Simulation and predicted accelerations are shown, with percent errors.

	Simulation PLA (g)	Acceleration as a Function of Deformation		Acceleration as a Function of Delta V	
		Predicted PLA (g)	Percent Error (%)	Predicted PLA (g)	Percent Error (%)
	62.0	18.0	-70.9	89.5	44.4
	31.1	21.7	-30.2	16.7	-46.3
Average			-50.6		-1.0

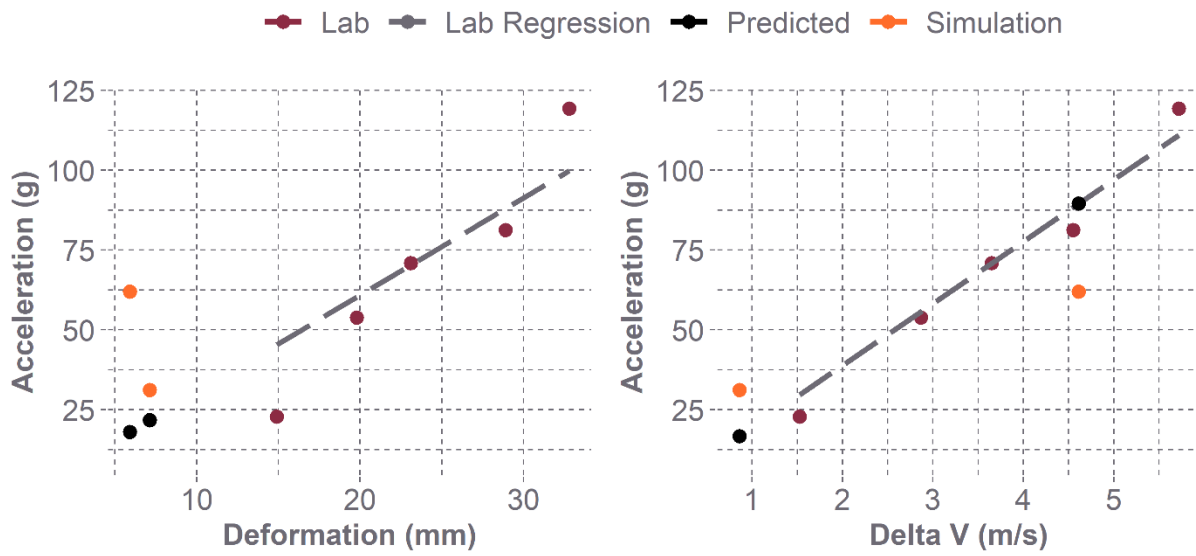


Figure 2.5 Acceleration as a function of deformation (left) and as a function of delta V (right) for the 21-degree impact condition. Simulation deformations were much lower than lab results, while delta Vs aligned well. Acceleration as a function of delta V was a better fit for the lab results, and overall predicted accelerations closer to simulation results.

Condition E

The DOF was approximated as 15°. This resulted in an impact to the lower right side of the helmet, just below and behind the edge of the face shield.

Simulation and Laboratory Results

Two simulations were selected to represent the 15-degree car impact condition. The DOF values were: 15.3° and 13.8°. Car resultant delta V values were: 14.5 m/s and 12.7 m/s. Table 2.6.a summarizes the simulation results for this condition. The laboratory testing results can be seen in Table 2.6.b. Simulation total deformations (19.22 mm, 18.55 mm) matched well with lab deformations (13.4 -29.7 mm). Simulation delta V values (5.85 m/s and 5.31 m/s) were slightly above the greatest lab delta V value (5.06 m/s).

Table 2.6.a Simulation results for the 15-degree impacts. Helmet, head surround, computed total, and measured total deformations were all reported. Head delta V and head PLA were also determined.

Car Impact DOF (°)	Delta V (m/s)	PLA (g)	Deformation (mm)			
			Helmet	Head Surround	Computed Total	Measured Total
15	5.85	48.9	2.99	17.24	19.19	19.22
15	5.31	44.8	2.82	16.46	18.52	18.55

Table 2.6.b The laboratory testing results for the 15-degree impacts. Total deformation was recorded, as well as impactor velocity, headform delta V, and headform PLA.

Car Impact DOF (°)	Impactor Velocity (m/s)	Delta V (m/s)	PLA (g)	Deformation (mm)
15	2.00	1.68	29.9	13.4
15	3.18	2.82	44.4	19.2
15	3.94	3.57	59.2	23.3
15	5.00	4.70	83.9	27.0
15	5.37	5.06	89.9	29.7

Regression Analysis Results

Regression analysis results for the 15-degree impacts are shown in Table 2.6.c. Acceleration was well predicted when deformation was the independent variable, with an average error of 13.0% from simulation values. Acceleration was overpredicted when delta V was the independent variable, with the predicted accelerations (101.5 g and 92.2 g) much larger than the simulation values (48.9 g and 44.8 g), resulting in an average error of 106.6%. Figure 2.6 shows acceleration as a function of deformation and acceleration as a function of delta V. The delta V-based regression model was a better fit for the lab results. However, the deformation-based model predicted values much closer to the simulation results.

Table 2.6.c Regression analysis results for the 15-degree impacts. Simulation and predicted accelerations are shown, with percent errors.

	Simulation PLA (g)	Acceleration as a Function of Deformation		Acceleration as a Function of Delta V	
		Predicted PLA (g)	Percent Error (%)	Predicted PLA (g)	Percent Error (%)
	48.9	53.8	10.1	101.5	107.6
	44.8	51.9	15.8	92.2	105.6
Average			13.0		106.6

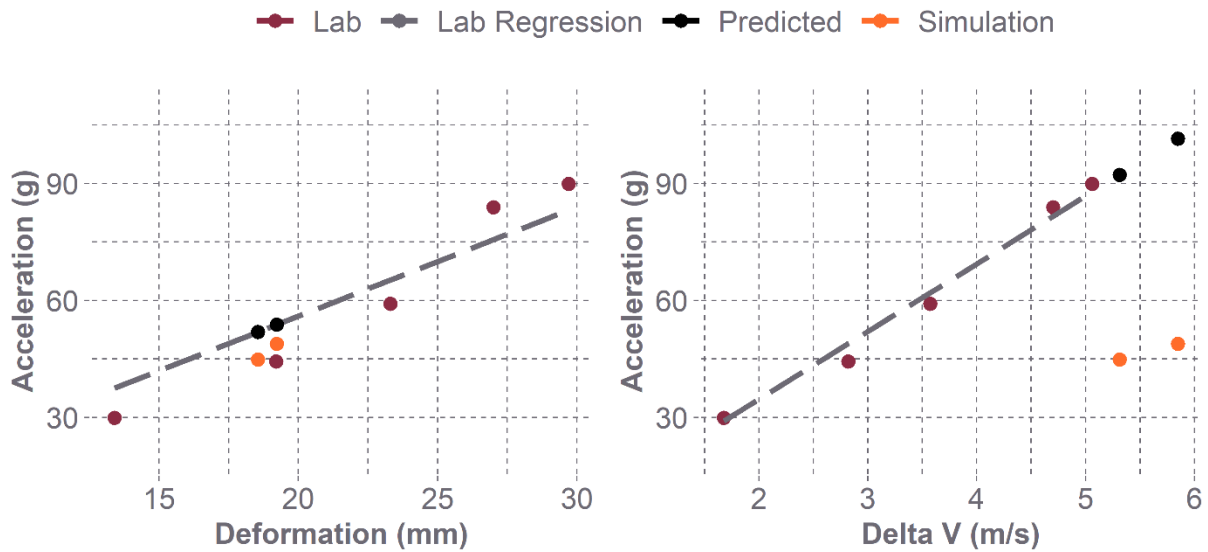


Figure 2.6 Acceleration as a function of deformation (left) and as a function of delta V (right) for the 15-degree impact condition. The delta V-based regression model was a better fit for the lab results. However, the deformation-based model predicted values much closer to the simulation results.

Condition F

The DOF was approximated as 9°. This resulted in an impact to the lower right side of the helmet, below and further forward than the 15-degree location.

Simulation and Laboratory Results

Four simulations were selected to represent the 9-degree impact. The simulation DOF values were: 2.7°, 8.2°, 0.3°, and 10.2°. Simulation car delta V values were: 67.6, 73.0, 58.0, 70.9 m/s. Table 2.7.a summarizes the simulation results, and the laboratory results are reported in Table 2.7.b. Simulation deformations (11.67 mm – 27.13 mm) aligned well with lab values (12.4 mm – 35.3 mm). Simulation delta V values exceeded lab values.

Table 2.7.a Simulation results for the 9-degree impacts. Helmet, head surround, computed total, and measured total deformations were all reported. Head delta V and head PLA were also determined.

Car Impact DOF (°)	Delta V (m/s)	PLA (g)	Deformation (mm)			
			Helmet	Head Surround	Computed Total	Measured Total
9	13.76	73.0	3.51	14.16	22.65	22.66
9	11.75	70.9	4.35	18.34	27.12	27.13
2	9.26	67.6	2.01	10.26	18.28	18.29
2	6.71	58.0	1.72	6.26	11.67	11.67

Table 2.7.b The laboratory testing results for the 9-degree impacts. Total deformation was recorded, as well as impactor velocity, headform delta V, and headform PLA.

Car Impact DOF (°)	Impactor Velocity (m/s)	Delta V (m/s)	PLA (g)	Deformation (mm)
9	1.85	1.47	19.5	12.4
9	3.24	2.79	37.1	20.8
9	3.69	3.26	40.4	23.3
9	5.13	4.72	59.3	29.4
9	6.19	5.97	90.8	35.3

Regression Analysis Results

Regression analysis results for the 9-degree impacts are shown in Table 2.7.c. Acceleration was underpredicted when deformation was the independent variable and overpredicted when based on delta V. The deformation-based model had a lower prediction error ($-38.0 \pm 16.1\%$), compared to the delta V model ($110.0 \pm 44.2\%$). Figure 2.7 shows acceleration as a function of deformation and acceleration as a function of delta V. Acceleration as a function of delta V was a slightly better fit for the lab results, but the error between the simulation and predicted accelerations was less when deformation was the predictor variable.

Table 2.7.c Regression analysis results for the 9-degree impacts. Simulation and predicted accelerations are shown, with percent errors.

	Simulation PLA (g)	Acceleration as a Function of Deformation		Acceleration as a Function of Delta V	
		Predicted PLA (g)	Percent Error (%)	Predicted PLA (g)	Percent Error (%)
	73.0	48.3	-33.9	190.5	160.9
	70.9	57.8	-18.5	162.7	129.4
	67.6	39.0	-42.3	128.2	89.7
	58.0	24.9	-57.1	93.0	60.2
Average			-38.0 ± 16.1		110.0 ± 44.2

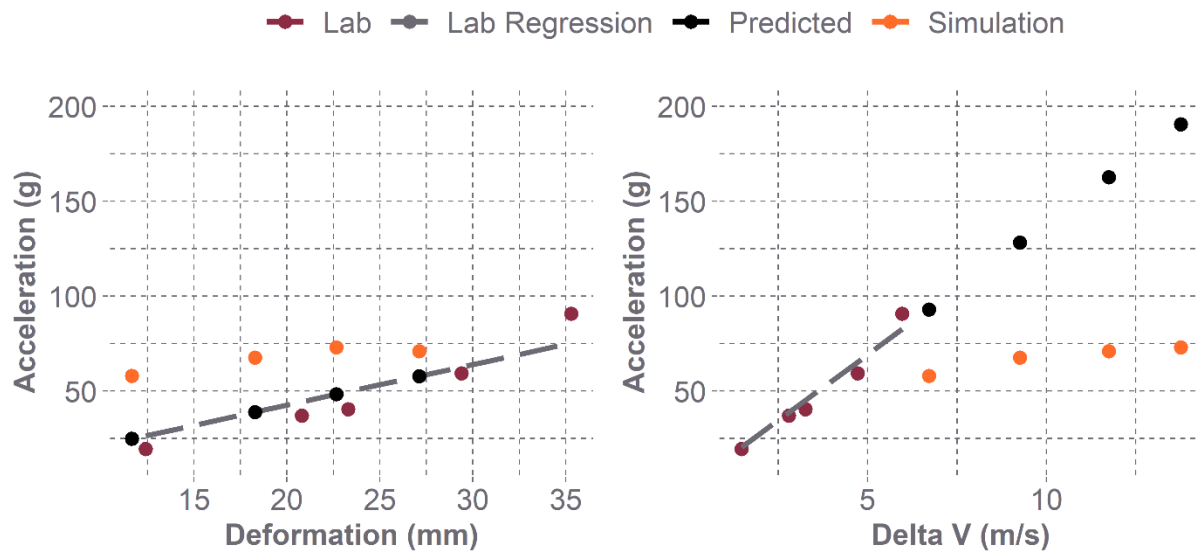


Figure 2.7 Acceleration as a function of deformation (left) and as a function of delta V (right) for the 9-degree impact condition. Acceleration as a function of delta V was a better fit for the lab results. However, the model using deformation as a predictor variable had less error between predicted and simulation results.

Condition G

The DOF was approximated as -9° . This resulted in an impact to the lower left side of the helmet, below and behind the edge of the face shield.

Simulation and Laboratory Results

Two simulations were chosen to represent this condition. The simulation DOF values were: -9.7° and -7.5° . The simulation delta V values were: 22.6 and 8.6 m/s. Table 2.8.a summarizes the simulation results, and the laboratory results are reported in Table 2.8.b. Simulation deformations (12.20 mm and 25.36 mm) aligned well with lab values (13.3 mm – 33.4 mm). Simulation head delta V values exceeded lab values.

Table 2.8.a Simulation results for the -9-degree impacts. Helmet, head surround, computed total, and measured total deformations were all reported. Head delta V and head PLA were also determined.

Car Impact DOF (°)	Delta V (m/s)	PLA (g)	Deformation (mm)			
			Helmet	Head Surround	Computed Total	Measured Total
-9	12.04	55.7	3.05	17.36	25.33	25.36
-9	4.53	37.8	0.95	7.07	12.18	12.20

Table 2.8.b The laboratory testing results for the -9-degree impacts. Total deformation was recorded, as well as impactor velocity, headform delta V, and headform PLA.

Car Impact DOF (°)	Impactor Velocity (m/s)	Delta V (m/s)	PLA (g)	Deformation (mm)
-9	1.98	1.53	22.4	13.3
-9	3.24	2.63	32.9	20.3
-9	4.04	3.51	42.3	26.1
-9	5.18	4.80	54.8	31.6
-9	6.08	5.82	80.0	33.4

Regression Analysis Results

Regression analysis results for the -9-degree impacts are shown in Table 2.8.c. Acceleration was underpredicted when deformation was the independent variable and overpredicted when based on delta V. Overall, the deformation condition had a smaller average error (-25.6%) than the delta V condition (113.5%). Figure 2.8 shows acceleration as a function of deformation and acceleration as a function of delta V. Acceleration as a function of delta V was a slightly better fit for the lab results, but the error between the simulation and predicted accelerations was much less when deformation was the predictor variable.

Table 2.8.c Regression analysis results for the -9-degree impacts. Simulation and predicted accelerations are shown, with percent errors.

	Simulation PLA (g)	Acceleration as a Function of Deformation		Acceleration as a Function of Delta V	
		Predicted PLA (g)	Percent Error (%)	Predicted PLA (g)	Percent Error (%)
	55.7	48.5	-12.9	153.0	174.8
	37.8	23.3	-38.3	57.6	52.3
Average			-25.6		113.5

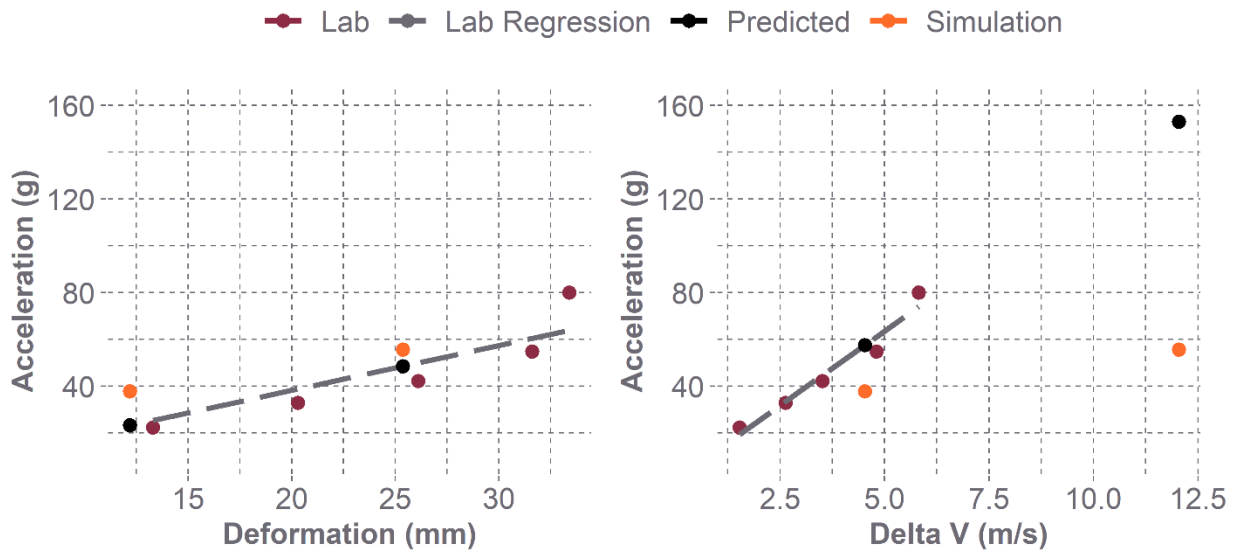


Figure 2.8 Acceleration as a function of deformation (left) and acceleration as a function of delta V (right) for the -9-degree impact condition. Acceleration as a function of delta V was a slightly better fit for the lab results, but the error between the simulation and predicted accelerations was much less when deformation was the predictor variable.

Condition H

The DOF was approximated as -21°. This resulted in an impact to the center of the left side of the helmet.

Simulation and Laboratory Results

Two simulations were chosen to represent this condition. The simulation DOF values were: -22.3° and -19.4°. The simulation delta V values were: 32.9 and 21.0 m/s. Table 2.9.a summarizes the simulation results, and the laboratory results are reported in Table 2.9.b. Simulation deformations (15.04 mm and 9.52 mm) aligned well with the lower lab values (12.3 mm – 18.1 mm). Simulation head delta V values were slightly greater than lab values.

Table 2.9.a Simulation results for the -21-degree impacts. Helmet, head surround, computed total, and measured total deformations were all reported. Head delta V and head PLA were also determined.

Car Impact DOF (°)	Delta V (m/s)	PLA (g)	Deformation (mm)			
			Helmet	Head Surround	Computed Total	Measured Total
-21	8.20	68.9	2.90	13.47	15.03	15.04
-21	5.47	54.5	2.31	7.94	9.51	9.52

Table 2.9.b The laboratory testing results for the -21-degree impacts. Total deformation was recorded, as well as impactor velocity, headform delta V, and headform PLA.

Car Impact DOF (°)	Impactor Velocity (m/s)	Delta V (m/s)	PLA (g)	Deformation (mm)
-21	1.96	1.69	28.3	12.3
-21	3.14	2.78	48.2	18.1
-21	4.08	3.65	64.6	23.0
-21	5.18	4.63	104.0	27.2
-21	6.19	5.64	119.2	33.3

Regression Analysis Results

Regression analysis results for the -21-degree impacts are shown in Table 2.9.c. Acceleration was underpredicted when deformation was used as the predictor, and overpredicted when delta V was used. The model using deformation produced smaller average error (-34.6%) than the delta V-based model (123.3%). Figure 2.9 shows acceleration as a function of deformation and acceleration as a function of delta V. The delta V-based model was a slightly better fit to the lab results, but the deformation-based model was a much better predictor than the delta-V model, with predicted accelerations much closer to the simulated values.

Table 2.9.c Regression analysis results for the -21-degree impacts. Simulation and predicted accelerations are shown, with percent errors.

	Simulation PLA (g)	Acceleration as a Function of Deformation		Acceleration as a Function of Delta V	
		Predicted PLA (g)	Percent Error (%)	Predicted PLA (g)	Percent Error (%)
	68.9	50.0	-27.4	166.8	142.1
	54.5	31.7	-41.9	111.4	104.5
Average			-34.6		123.3

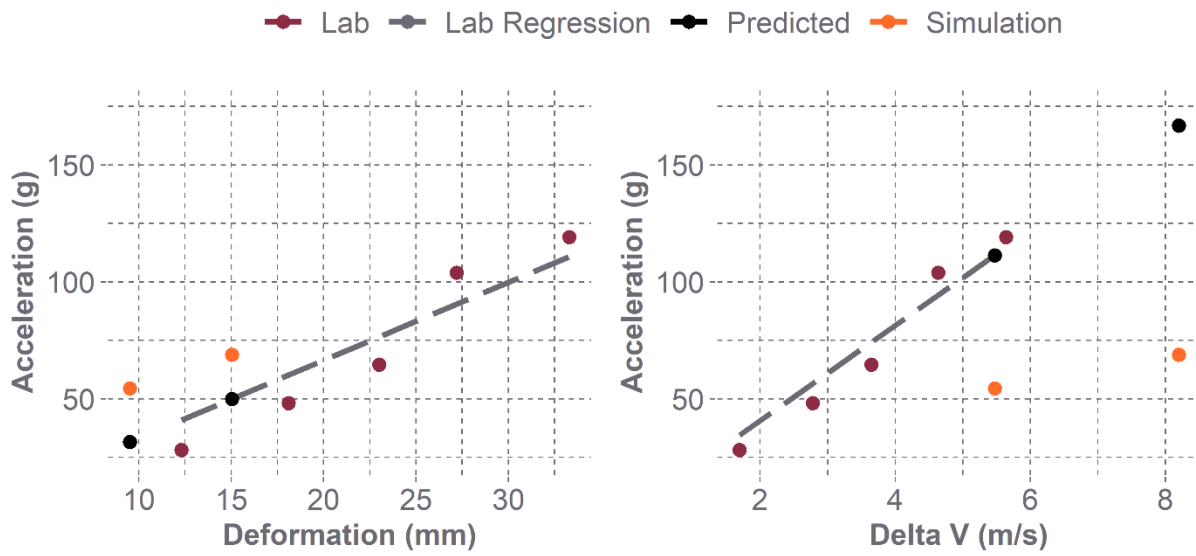


Figure 2.9 Acceleration as a function of deformation (left) and acceleration as a function of delta V (right) for the -21-degree impact condition. The delta V-based model was a slightly better fit to the lab results, but the deformation-based model was a much better predictor than the delta-V model, with predicted accelerations much closer to the simulated values.

Condition I

The DOF was approximated as -55°. This resulted in an impact to the left rear boss region of the helmet.

Simulation and Laboratory Results

Two simulations were chosen to represent this condition. The simulation DOF values were: -53.8° and -56.8°. The simulation delta V values were: 30.2 and 26.7 m/s. Table 2.10.a summarizes the simulation results, and the laboratory results are reported in Table 2.10.b. Simulation deformations (10.24 mm and 11.21 mm) were below the lowest lab value (15.0 mm). Simulation head delta V values were slightly below the lowest lab value as well.

Table 2.10.a Simulation results for the -55-degree impacts. Helmet, head surround, computed total, and measured total deformations were all reported. Head delta V and head PLA were also determined.

Car Impact DOF (°)	Delta V (m/s)	PLA (g)	Deformation (mm)			
			Helmet	Head Surround	Computed Total	Measured Total
-55	1.93	68.2	1.07	9.72	10.24	10.24
-55	1.76	57.0	1.20	10.58	11.20	11.21

Table 2.10.b The laboratory testing results for the -55-degree impacts. Total deformation was recorded, as well as impactor velocity, headform delta V, and headform PLA.

Car Impact DOF (°)	Impactor Velocity (m/s)	Delta V (m/s)	PLA (g)	Deformation (mm)
-55	1.94	1.71	58.7	15.0
-55	3.29	2.93	63.3	19.0
-55	4.13	3.60	67.6	22.3
-55	5.00	4.42	99.8	25.8
-55	6.23	5.46	155.2	31.0

Regression Analysis Results

Regression analysis results for the -55-degree impacts are presented in Table 2.10.c. Both models underpredicted acceleration, and the average percent error was similar between the deformation condition (-29.7%) and the delta V condition (-27.2%). Figure 2.10 shows acceleration as a function of deformation and acceleration as a function of delta V. Both models fit the lab data well and had similar percent error between the predicted and simulation results.

Table 2.10.c Regression analysis results for the -55-degree impacts. Simulation and predicted accelerations are shown, with percent errors.

	Simulation PLA (g)	Acceleration as a Function of Deformation		Acceleration as a Function of Delta V	
		Predicted PLA (g)	Percent Error (%)	Predicted PLA (g)	Percent Error (%)
	68.2	41.5	-39.1	47.6	-30.2
	57.0	45.4	-20.3	43.3	-24.1
Average			-29.7		-27.2

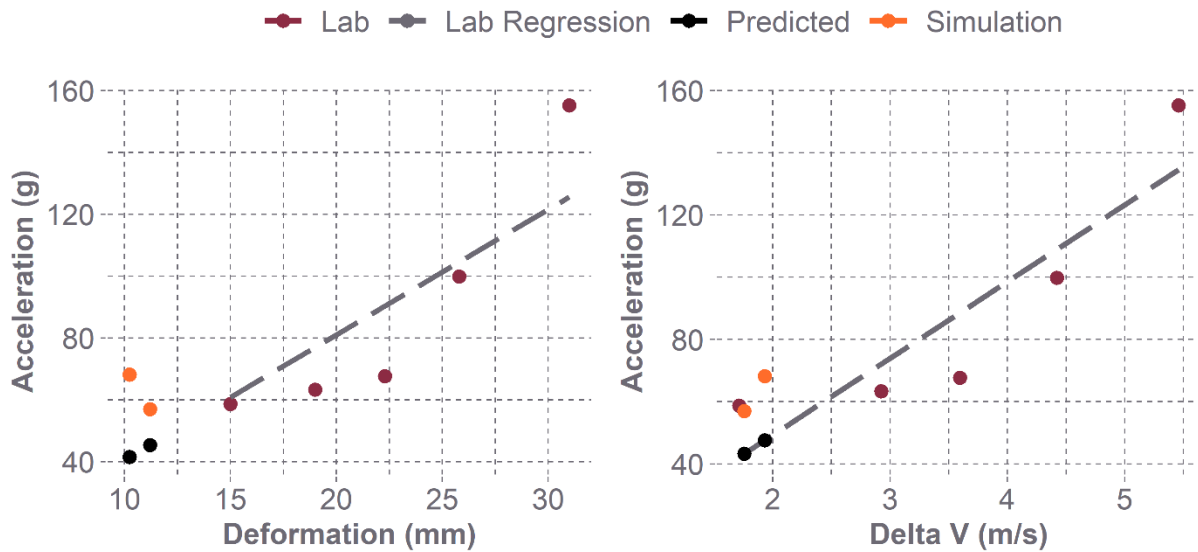


Figure 2.10 Acceleration as a function of deformation (left) and acceleration as a function of delta V (right) for the -55-degree impact condition. Both models fit the lab data well and had similar percent error between the predicted and simulation results.

Condition J

The DOF was approximated as -74°. This resulted in an impact to the left rear boss region of the helmet. This location was slightly farther behind and higher than the -55 center of impact.

Simulation and Laboratory Results

Two simulations were identified to represent this condition. The simulation DOF values were: -72.3° and -74.9°. The simulation delta V values were: 19.0 m/s and 19.9 m/s. Table 2.11.a summarizes the simulation results, and the laboratory results are reported in Table 2.11.b. Simulation deformations were below lab results. Simulation delta V values (2.45 m/s and 1.57 m/s) aligned well with the lower lab values (1.72 m/s and 2.78 m/s).

Table 2.11.a Simulation results for the -74-degree impacts. Helmet, head surround, computed total, and measured total deformations were all reported. Head delta V and head PLA were also determined.

Car Impact DOF (°)	Delta V (m/s)	PLA (g)	Deformation (mm)			
			Helmet	Head Surround	Computed Total	Measured Total
-74	2.45	38.9	1.30	7.47	8.93	8.94
-74	1.57	38.3	1.23	6.80	8.37	8.38

Table 2.11.b The laboratory testing results for the -74-degree impacts. Total deformation was recorded, as well as impactor velocity, headform delta V, and headform PLA.

Car Impact DOF (°)	Impactor Velocity (m/s)	Delta V (m/s)	PLA (g)	Deformation (mm)
-74	1.99	1.72	80.3	14.9
-74	3.04	2.78	82.8	19.9
-74	4.13	3.73	62.9	24.9
-74	5.18	4.72	87.8	29.9
-74	6.23	5.67	119.3	33.5

Regression Analysis Results

Regression analysis results for the -74-degree impacts are reported in Table 2.11.c. Acceleration was slightly underpredicted when deformation was the predictor. When delta V was the predictor, predicted acceleration values (52.5 g and 33.7 g) were slightly above and below simulation values (38.9 g and 38.3 g), respectively. The percent errors for both models were small. Figure 2.11 shows acceleration as a function of deformation and acceleration as a function of delta V. The deformation-based model was a slightly better fit to lab results than the delta V-based model. The average percent errors between the predicted and simulation results were small for both models, with the delta V-based model performing slightly better.

Table 2.11.c Regression analysis results for the -74-degree impacts. Simulation and predicted accelerations are shown, with percent errors.

	Simulation PLA (g)	Acceleration as a Function of Deformation		Acceleration as a Function of Delta V	
		Predicted PLA (g)	Percent Error (%)	Predicted PLA (g)	Percent Error (%)
	38.9	30.3	-22.2	52.5	34.9
	38.3	28.4	-25.8	33.7	-12.0
Average			-24.0		11.4

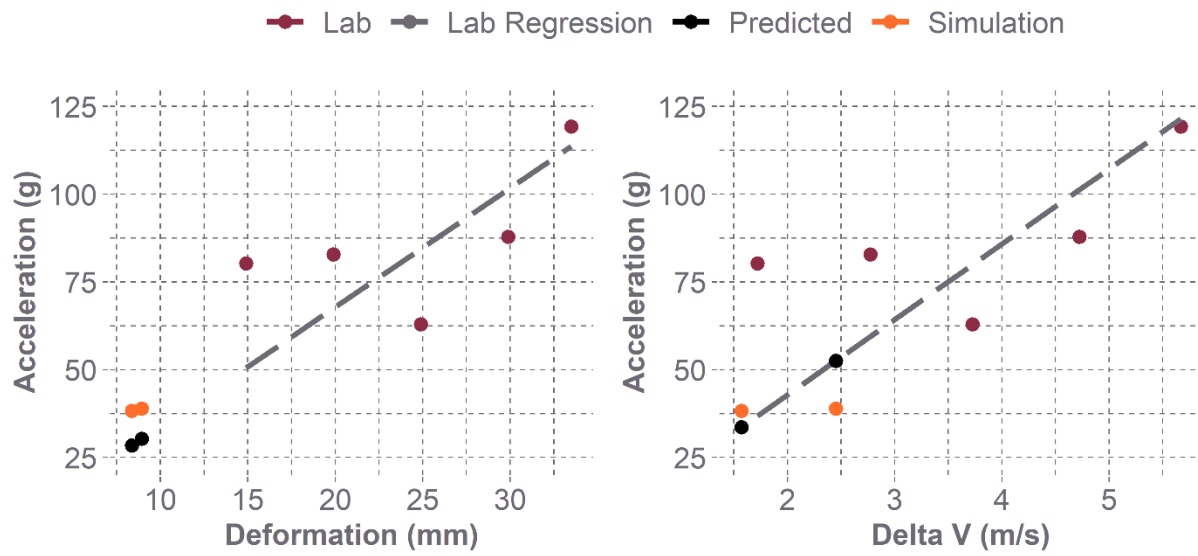


Figure 2.11 Acceleration as a function of deformation (left) and acceleration as a function of delta V (right) for the -74-degree impact condition. The deformation-based model was a slightly better fit to lab results. The average percent errors between the predicted and simulation results were small for both models, with the delta V-based model performing slightly better.

Discussion

In this study, we compared simulations to laboratory tests, based on acceleration, velocity, and deformation, for the evaluation of motorsport helmets. Computational models of full-sled collisions were used to identify criteria for the test series, including impact locations, impact speed, and desired acceleration range. The laboratory test series aimed to represent an isolated head impact event. The laboratory tests were then compared to the simulation head impact event, isolated within the overall simulation crash. In order to isolate the head event from the longer, more complex full crash pulse, deformation and delta V were identified as primary metrics. Deformation and delta V are used as correlates to understand the energy transferred to the head, without needing to separate multiple impact pulse components. The associated accelerations were also used to compare the simulation and laboratory head impacts.

For the simulation impacts, energy was managed by both the helmet and head surround, whereas the laboratory tests used a much more rigid system, with a small amount of padding placed on the impactor, and the helmet managing most of the energy. Lab-based helmet testing procedures are typically done with a rigid system in order to highlight helmet performance. A small amount of padding was used in order to extend the impact duration and be more similar to the simulation impacts, while still highlighting helmet performance. However, the differences in systems and the amount of padding involved will still result in some differences in how the impact energy is managed.

Overall, the average simulation total deformation (7.26 ± 2.27 mm) was less than the average of the minimum lab deformation (15.67 ± 1.22 mm) for six of the ten locations (21° , 37° , 54° , 75° , -55° , -74°). These locations were all on the side and rear boss regions of the helmet, whereas the four locations that experienced similar average simulation (17.96 ± 5.92 mm) and lab deformations (23.62 ± 7.34 mm) were at the front side regions of the helmet. Additionally, the simulation computed total deformation and measured total deformation were very similar, with a mean difference of 0.01 ± 0.008 mm. Simulation helmet deformations had an average of 1.9 ± 0.94 mm and were generally much lower than lab deformations. The greatest simulation helmet deformations were in the 9° condition (3.51 mm and 4.35 mm) and 15° condition (2.99 mm and 2.82 mm). The simulation head surround deformations had some overlap with lab deformations, and had an average of 8.9 ± 4.8 mm. The greatest head surround deformations again occurred in the 9° (14.16 mm and 18.34 mm) and 15° conditions (17.24 mm and 16.46 mm). Overall, this highlights that impacts on the more frontal regions of the helmet experienced greater deformations for each simulation component, and the total deformations were similar to the lab deformations.

This makes sense, because these frontal locations tended to have smaller impact regions on the head surround and had longer impact durations.

The simulation delta V values had a larger range than the lab results, but the average simulation delta V (4.49 ± 3.94 mm) was similar to the lab results (3.65 ± 1.63 mm). Four locations (75° , 54° , -55° , -74°) at the rear region of the helmet had simulation values within the lower range of lab values. Meanwhile four locations at the front region of the helmet (15° , 9° , -9° , -21°) had simulation delta V that were within and above the upper range of lab values. Two locations (37° , 21°) had simulation values slightly below lab values.

Linear relationships between the lab variables were consistently observed. Both deformation (average $R^2 = 0.962$) and delta V (average $R^2 = 0.982$) were good predictors of head acceleration. Average percent errors between the simulation accelerations and the simulation-matched predicted accelerations were compared for each predictor variable. The deformation-based model was, therefore, best suited for estimating accelerations when the impact locations were toward the front of the helmet. The delta V-based model was best suited for estimating accelerations when the impact locations were toward the rear of the helmet.

For the deformation-based model, average error was $-35.7 \pm 24.2\%$, indicating that it consistently underpredicted accelerations. Seven of the ten locations (75° , 15° , 9° , -9° , -21° , -55° , -74°) were below an average error of 40%, with the 9° condition reporting the highest value of $-38.0 \pm 16.1\%$. The overall highest average error for this model was seen for the 37° condition (-75.5%). High average errors were seen in conditions that had simulation deformations that were substantially less than the lab deformations used to create the linear regression, such as 54° , 37° , and 21° . Additionally, these low simulation deformations corresponded to accelerations that were greater than the lab accelerations for matched deformation values.

For the delta V-based model, average error was $36.7 \pm 76.0\%$. This indicates that the model consistently overpredicted accelerations. It also had higher average error than the deformation-based model, and a greater range of error. The lowest average error was -1.0% , and was observed in the 21° degree condition. Six locations had absolute average errors below 42.6% . The highest errors were seen in frontal impact conditions (15° , 9° , -9° , and -21°) with errors of (106.6% , $110.0 \pm 44.2\%$, 113.5% , and 123.3%). The high errors seen in these frontal locations could be in part because they experienced greater delta V values than the range of lab values used to create the linear regression. Additionally, these conditions experienced high delta V values, with high deformation values, but the corresponding accelerations were much lower than lab accelerations for matched or lower delta V values.

When this is all considered together, it is clear that locations at the front regions of the helmet had simulation deformations within similar ranges of the lab deformations, delta V values larger than the corresponding lab values, and accelerations lower than the corresponding lab and predicted values. Meanwhile, locations at the rear regions of the helmet experienced simulation deformations below the lab results, delta V values that matched the lower range of lab values, and accelerations that were within the lower range of laboratory accelerations. These differences can likely be explained due to the helmet interaction with the head surround in the simulations. For example, a rear boss center of impact would strike the head surround, causing small amounts of deformation, before the impact DOF would cause it to “roll” along the head surround during impact. This also resulted in the impact duration at the initial center of impact to be shorter, when compared to other DOF conditions. This produced low delta V values and accelerations. Alternatively, a frontal impact would strike the front region of the head surround and would experience less “rolling”. This would produce a longer duration impact, concentrated on a smaller

region of the head surround, resulting in greater deformations and delta V values, and low acceleration experienced by the head. These examples highlight the large effect the head surround has in managing the impact energy.

The results of this study raise many considerations for a future helmet test protocol. First, the simulation data results indicate that the impact events are not very severe, in terms of the acceleration experienced by the head, when compared to the laboratory acceleration results. However, the similar delta V values between the simulation and laboratory results indicate that the energy managed by each system was similar, and highlights the fact that the protection systems within the car, such as the head surround and HANS device, are managing a large portion of the impact energy. This is important to consider for the purposes of a lab test which should effectively isolate the helmet, in order to reflect the helmet performance without contributions from other protective components that might conceal helmet deficiencies. Delta V and deformation were compared for the simulations and laboratory tests, in order to isolate the energy needed to be managed during each impact.

There was a large discrepancy between simulation and laboratory accelerations, again indicating how effectively the protective systems within the simulations were managing the impact energy. However, much more severe impacts are possible, such as the simulations that were removed from this study for having impact change in velocities greater than 60 kph (16.67 m/s). Additionally, the impact velocities used in the lab and the associated accelerations were below the 200 g thresholds listed in the Snell helmet standards [3]. The current simulation results would therefore serve as a lower bound for testing considerations. While the car protective systems are clearly effective, they should not be included in lab testing. This would make highlighting helmet

performance difficult, and would not enable meaningful acceleration comparisons in the context of injury risk.

We therefore suggest a simplified test based on the upper bounds of the energy involved in the head impact events considered in this study, as well as higher realistic head impact events. Some padding should be included on the impactor, in order to extend impact duration closer to real-world collision impacts, but also in order to limit accelerations from reaching unrealistically high values. This padding should not be so thick that it manages more energy than the helmet, which occurred in the simulation results. This will reduce impact duration compared to real-world events, but this is a necessary sacrifice for properly evaluating helmet performance on its own. Impact locations around the entire helmet circumference and within a realistic elevation range should be evaluated. Symmetry in impact locations should not be assumed due to differences in the car interior structure, such as the head surround. Impact locations around the helmet will help to ensure helmet integrity and a proper representation of real-world crash distributions. Additionally, any attachment points of helmet modifications should be included as test sites, in order to evaluate their effect on helmet performance in the event of an unpredictable impact location or scenario. Lastly, the protocol should be expanded to other impact scenarios that include a 5th percentile female and 95th percentile male headform and simulation model. Driver stature may alter how the driver fits within the car and could increase the likelihood of impacting the steering wheel and other car structures.

There were several limitations in this study. As discussed, the differences between a head impact in the laboratory and an isolated head impact event from within a full-sled simulation impact create challenges when comparing results. It is important to consider these differences when comparing how energy is managed in the systems, and that it is not an exact comparison.

Additionally, laboratory tests involved a linear impact in which deformation occurred in one location. This was assumed to be true in the simulation deformation analysis as well. However, the helmet tended to roll along the head surround during impact, changing the location of deformation. This effect was more apparent in some impact locations than others, and it was not accounted for in this study. Head surround deformation was instead averaged between two points within the same general region. There are also differences between the simulation helmet model used, which was a generalized helmet model, and the specific HJC helmet model used in the lab tests. This affects how helmet performance is compared and how the impact energy was managed. Lastly, aspects of this process involved making selections partly based on visual inspections. This process can introduce error, but the error was minimized by using a specific and consistent approach to making selections. Overall, these results offer valuable insight for comparing motorsport simulations and laboratory head impact events, and they should be considered when establishing future motorsport helmet testing protocols.

Conclusion

The purpose of this study was to compare simulation data to laboratory tests intended to simulate motorsport head impact events. In order to compare the simulations and lab tests the head impact event needed to be isolated. Deformation and delta V were calculated for the simulations and laboratory tests and used as correlates to isolate the head impact and compare the energy managed. Simulation deformations were generally less than the lab deformations, while delta V was aligned well with the lab results. Linear relationships were established between deformation and acceleration and delta V and acceleration for the lab results. These regressions were used to estimate lab kinematics based on simulation-matched predictors. The deformation-based model was best suited for estimating accelerations when impacts occurred along the front side region of

the helmet, whereas the delta V-based model was a better predictor for impacts along the rear boss region of the helmet. The lab results generally tested higher severity impacts with higher accelerations, while the simulation crashes experienced low kinematics. The energy managed was similar for both the lab and simulations results, indicating a large amount of the energy involved in the simulations was managed by the protective systems. These findings help to inform future helmet testing protocols in order to better match real-world simulations.

References

- [1] A. Kaul, A. Abbas, G. Smith, S. Manjila, J. Pace, and M. Steinmetz, "A revolution in preventing fatal craniovertebral junction injuries: lessons learned from the Head and Neck Support device in professional auto racing," *Journal of neurosurgery: Spine*, vol. 25, no. 6, pp. 756-761, 2016.
- [2] J. Patalak, T. Gideon, and J. Melvin, "Examination of a properly restrained motorsport occupant," *SAE International journal of transportation safety*, vol. 1, no. 2, pp. 261-277, 2013.
- [3] *Special Applications Standard for Protective Headgear: For Use in Competitive Automotive Sports*, I. The Snell Foundation, 2020. [Online]. Available: http://smf.org/standards/sa/2020/SA2020_final.pdf
- [4] *SFI Specification 38.1*, I. SFI Foundation, 2019. [Online]. Available: https://www.sfifoundation.com/wp-content/pdfs/specs/Spec_38.1_041919.pdf
- [5] *SFI Specification 41.1*, I. SFI Foundation, 2013. [Online]. Available: https://www.sfifoundation.com/wp-content/pdfs/specs/Spec_41.1_032713.pdf
- [6] *SFI Specification 45*, I. SFI Foundation, 2013. [Online]. Available: https://www.sfifoundation.com/wp-content/pdfs/specs/Spec_45.2_032713.pdf
- [7] J. P. Patalak, M. G. Harper, A. A. Weaver, N. M. Dalzell, and J. D. Stitzel, "Estimated crash injury risk and crash characteristics for motorsport drivers," *Accident Analysis & Prevention*, vol. 136, p. 105397, 2020.
- [8] N. D. Deakin *et al.*, "Concussion in motor sport: a medical literature review and engineering perspective," *Journal of Concussion*, vol. 1, p. 2059700217733916, 2017.
- [9] O. Minoyama and H. Tsuchida, "Injuries in professional motor car racing drivers at a racing circuit between 1996 and 2000," (in English), *British Journal of Sports Medicine*, vol. 38, no. 5, p. 613, Oct 2004, 2016-04-07 2004, doi: <http://dx.doi.org/10.1136/bjism.2003.007674>.
- [10] S. A. Adams, A. P. Turner, H. Richards, and P. J. Hutchinson, "Concussion in motorsport? Experience, knowledge, attitudes, and priorities of medical personnel and drivers," *Clinical journal of sport medicine*, vol. 30, no. 6, pp. 568-577, 2020.
- [11] R. C. Butz, B. M. Knowles, J. A. Newman, and C. R. Dennison, "Effects of external helmet accessories on biomechanical measures of head injury risk: An ATD study using the HYBRIDIII headform," *Journal of biomechanics*, vol. 48, no. 14, pp. 3816-3824, 2015.
- [12] W. B. Decker, D. A. Jones, K. Devane, M. L. Davis, J. P. Patalak, and F. S. Gayzik, "Simulation-based assessment of injury risk for an average male motorsport driver," *Traffic Injury Prevention*, pp. 1-6, 2020, doi: 10.1080/15389588.2020.1802021.

Appendix A: Summary Tables for Simulation and Laboratory Results

Table A.1 Summary table of all metrics calculated for the simulation impacts. Impacts were grouped based on the direction of force (DOF) of the simulation impact. Head kinematics, Head Injury Criterion (HIC) 15 ms, and multiple deformation measurements were found.

DOF (Degrees)	Delta V (m/s)	PLA (g)	Deformation (mm)				PRV (rad/s)	HIC15
			Helmet	Surround	Computed Total	Measured Total		
70	1.85	46.8	1.21	5.37	6.79	6.80	15.4	112.6
75	2.29	42.9	1.50	6.61	8.34	8.35	13.6	101.6
70	1.65	27.9	1.03	4.69	5.92	5.93	10.1	30.1
75	2.09	43.8	1.38	8.07	9.55	9.56	14.5	109.6
54	1.14	37.1	1.08	3.52	4.85	4.85	16.1	73.1
54	1.51	67.0	1.20	4.72	6.22	6.22	19.7	303.1
37	0.52	52.2	1.13	3.45	4.57	4.58	16.9	216.4
37	0.69	49.0	1.12	2.29	3.52	3.52	15.5	176.4
21	4.61	62.0	2.10	5.37	5.92	5.93	13.5	289.8
21	0.86	31.1	1.52	6.18	7.13	7.14	9.4	25.1
15	5.85	48.9	2.99	17.24	19.19	19.22	10.6	136.8
15	5.31	44.8	2.82	16.46	18.52	18.55	9.8	109.5
9	13.76	73.0	3.51	14.16	22.65	22.66	14.0	440.0
9	11.75	70.9	4.35	18.34	27.12	27.13	15.6	453.6
9	9.26	67.6	2.01	10.26	18.28	18.29	14.5	352.5
9	6.71	58.0	1.72	6.26	11.67	11.67	11.0	237.2
-9	12.04	55.7	3.05	17.36	25.33	25.36	12.7	249.1
-9	4.53	37.8	0.95	7.07	12.18	12.20	7.4	54.4
-21	8.20	68.9	2.90	13.47	15.03	15.04	18.1	463.8
-21	5.47	54.5	2.31	7.94	9.51	9.52	14.1	225.6
-55	1.93	68.2	1.07	9.72	10.24	10.24	24.7	336.0
-55	1.76	57.0	1.20	10.58	11.20	11.21	22.9	216.1
-74	2.45	38.9	1.30	7.47	8.93	8.94	14.7	78.6
-74	1.57	38.3	1.23	6.80	8.37	8.38	15.6	82.2

Table A.2 Summary table of all metrics calculated for the laboratory impacts. Impacts were grouped based on the direction of force (DOF) of the corresponding simulations. Head kinematics, Head Injury Criterion (HIC) 15 ms, and deformation were found.

DOF (degrees)	Impact Vel (m/s)	Delta V (m/s)	PLA (g)	Deformation (mm)	PRV (rad/s)	HIC15
75	1.98	1.66	22.8	14.9	10.0	10.1
75	3.16	2.85	56.6	19.3	16.9	48.7
75	3.98	3.70	95.0	21.8	22.6	106.8
75	5.05	4.81	91.1	27.6	28.7	247.6
75	6.12	5.72	127.8	30.3	35.8	494.7
54	1.78	1.39	29.4	17.8	8.8	6.6
54	2.57	2.24	42.3	21.5	13.8	23.6
54	3.75	3.43	56.3	23.4	22.2	82.9
54	4.95	4.73	118.1	29.2	29.9	217.6
54	6.08	5.50	117.8	30.1	36.7	459.4
37	2.00	1.74	26.0	16.5	10.6	12.5
37	3.18	2.93	45.1	19.7	18.5	51.6
37	4.05	3.71	67.1	23.1	32.3	116.6
37	5.08	4.70	94.7	27	37.7	242.0
37	6.08	5.47	114.0	32.3	37.7	403.5
21	1.80	1.53	22.9	14.9	10.0	8.8
21	3.17	2.87	53.8	19.8	18.2	50.8
21	4.00	3.65	70.9	23.1	22.8	102.7
21	4.90	4.55	81.3	28.9	28.2	191.7
21	6.16	5.72	119.4	32.8	37.3	381.6
15	2.00	1.68	29.9	13.4	9.8	11.8
15	3.18	2.82	44.4	19.2	17.3	43.9
15	3.94	3.57	59.2	23.3	23.1	85.1
15	5.00	4.70	83.9	27	30.3	189.7
15	5.37	5.06	89.9	29.7	33.5	237.7
9	1.85	1.47	19.5	12.4	8.0	6.4
9	3.24	2.79	37.1	20.8	18.2	35.7
9	3.69	3.26	40.4	23.3	21.7	52.3
9	5.13	4.72	59.3	29.4	32.0	154.1
9	6.19	5.97	90.8	35.3	40.7	337.7
-9	1.98	1.53	22.4	13.3	9.5	9.0
-9	3.24	2.63	32.9	20.3	16.4	29.6
-9	4.04	3.51	42.3	26.1	22.2	60.0
-9	5.18	4.80	54.8	31.6	32.7	134.7
-9	6.08	5.82	80.0	33.4	39.2	274.9

Table A.2 (Continued) Summary table of all metrics calculated for the laboratory impacts. Impacts were grouped based on the direction of force (DOF) of the corresponding simulations. Head kinematics, Head Injury Criterion (HIC) 15 ms, and deformation were found.

DOF (degrees)	Impact Vel (m/s)	Delta V (m/s)	PLA (g)	Deformation (mm)	PRV (rad/s)	HIC15
-21	1.96	1.69	28.3	12.3	10.9	13.4
-21	3.14	2.78	48.2	18.1	17.2	53.1
-21	4.08	3.65	64.6	23	22.7	113.4
-21	5.18	4.63	104.0	27.2	29.4	214.6
-21	6.19	5.64	119.2	33.3	36.1	369.5
-55	1.94	1.71	58.7	15	11.8	12.0
-55	3.29	2.93	63.3	19	21.1	57.5
-55	4.13	3.60	67.6	22.3	26.1	115.7
-55	5.00	4.42	99.8	25.8	32.5	223.0
-55	6.23	5.46	155.2	31	39.7	437.3
-74	1.99	1.72	80.3	14.9	10.5	10.7
-74	3.04	2.78	82.8	19.9	21.1	41.9
-74	4.13	3.73	62.9	24.9	23.8	115.5
-74	5.18	4.72	87.8	29.9	30.6	242.5
-74	6.23	5.67	119.3	33.5	35.9	454.1